HIGH FIELD NANOPLASMONICS
(AND SOME APPLICATIONS)

Norbert Kroo
Wigner Physics Research Center and
Hungarian Academy of Sciences

Motto: Only those, who are prepared to go too far, can know how far they may go.

PARTICLES AND PLASMAS 2022.05.17

FROM PETAWATTS TO NANOWATTS AND CW TO ATTOSECS

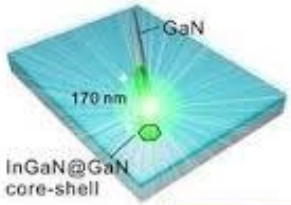

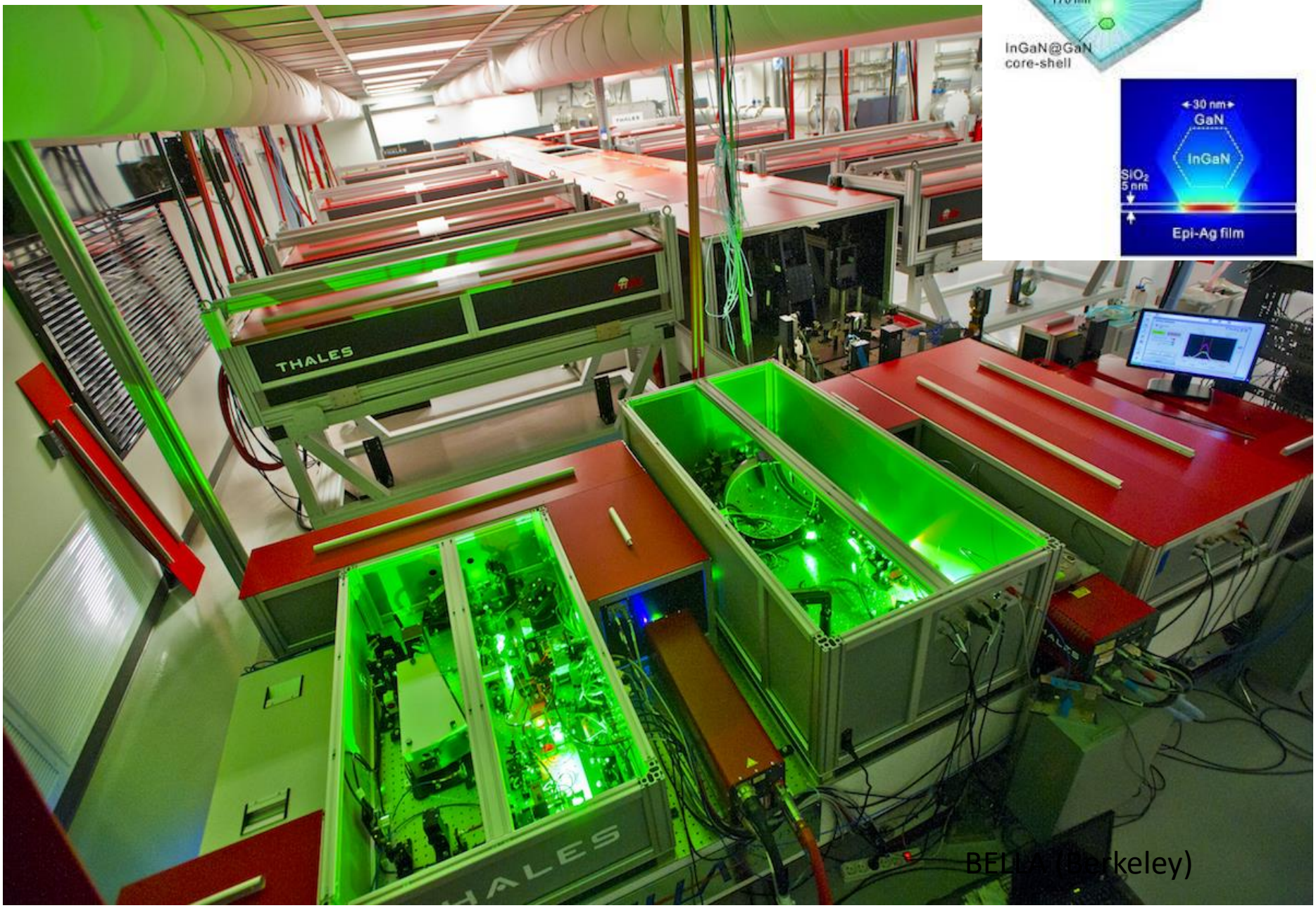

BELLA (Berkeley)

AND THE INCREASING INTENSITIES

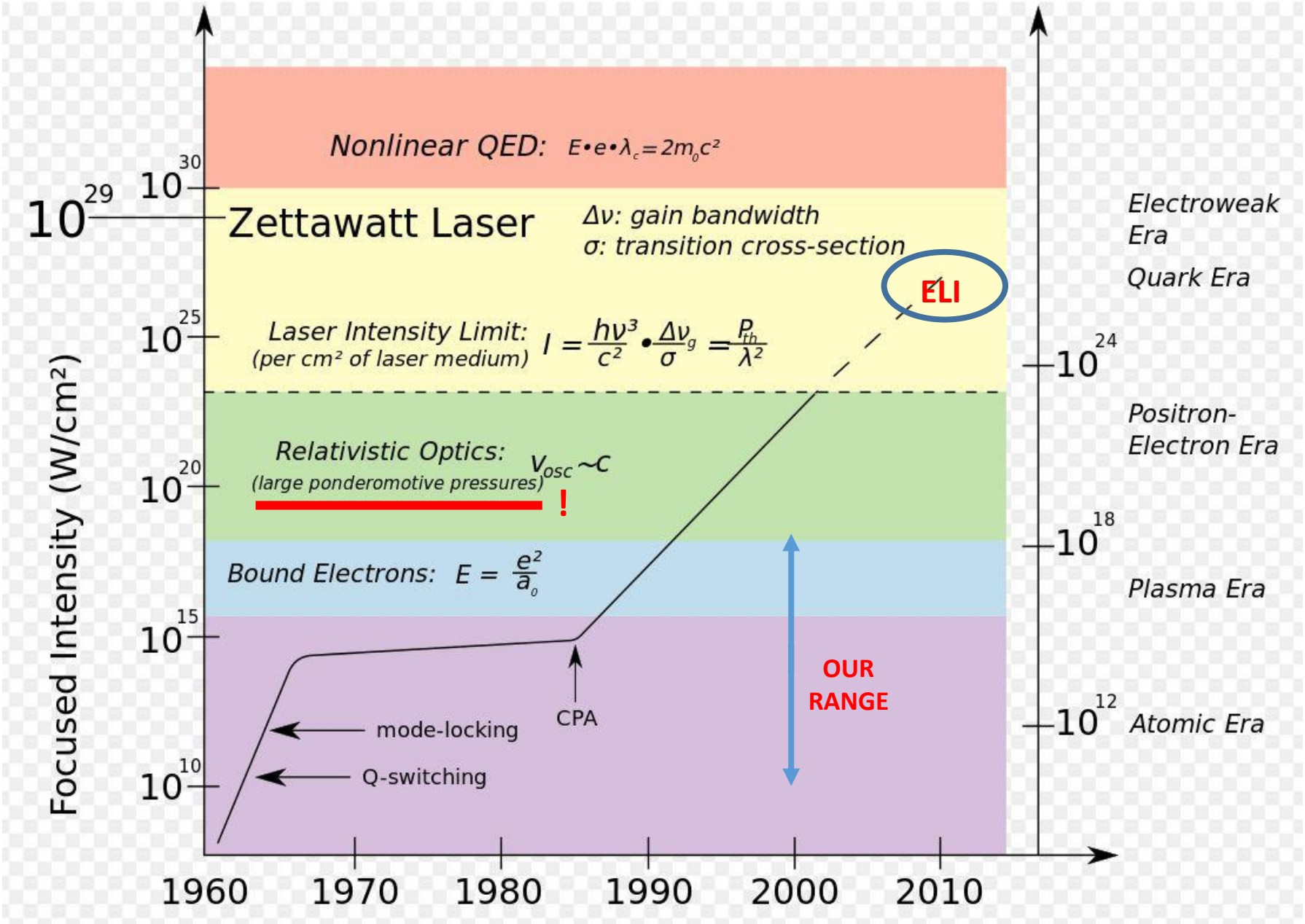

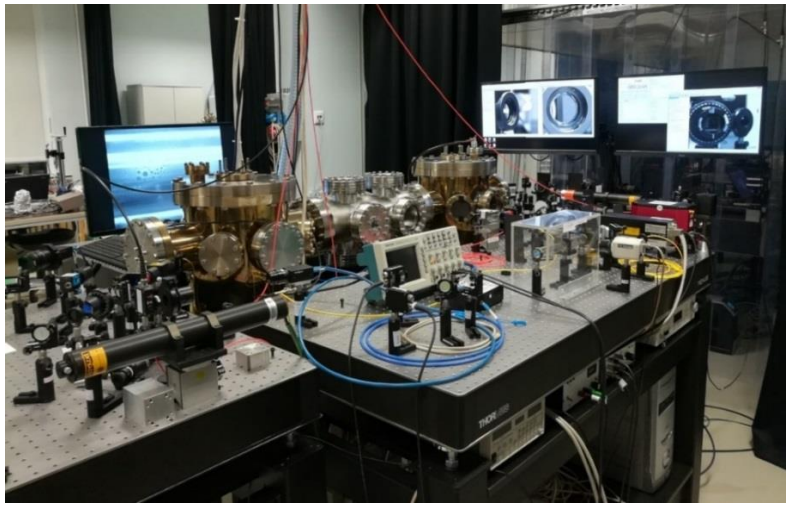

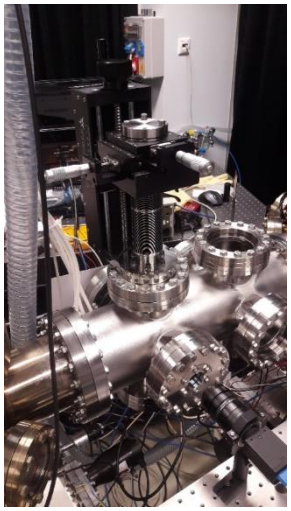

Ti::Sa laser:
800nm, 40fs
Max 30mJ
~10^{17} W/cm^2
Contrast ~ 10^6

THE OPTICAL NEAR FIELD

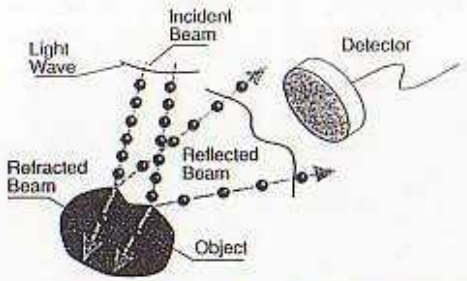

Schematic of the interaction between an object and a light beam. In first approximation, the light beam can be considered as projectiles launched against a target (the object) and then reflected towards the detector. This interpretation is primitive but provides the basis for the understanding of the notion of image.

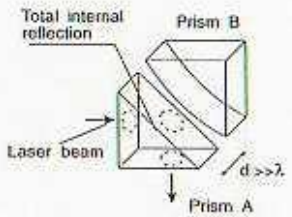

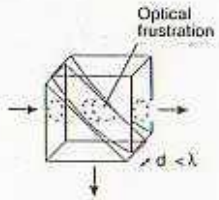

The famous experiment of Newton. A light beam is projected onto a prism. As expected, the beam is internally and totally reflected on the larger side of the prism. If a second prism is brought to the first one, no effect is detected unless the distance between the two prisms becomes smaller than a fraction of a micron. The light beam then seems to be captured by the second prism, frustrating the total reflection. The beam intensity transmitted through the second prism depends exponentially on the distance *d*.

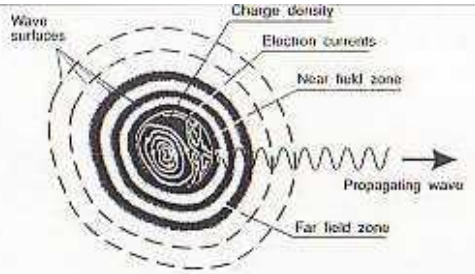

Field emitted from an object. The electron currents (in the case of conducting materials) and the charge densities inside the object induce an electromagnetic field radiating from the surface. Far away from the surface the field has the well known structure of propagating waves. Very close to the object (the region of the question mark), the field has a more complex structure since it is composed of propagating and non-radiating components.

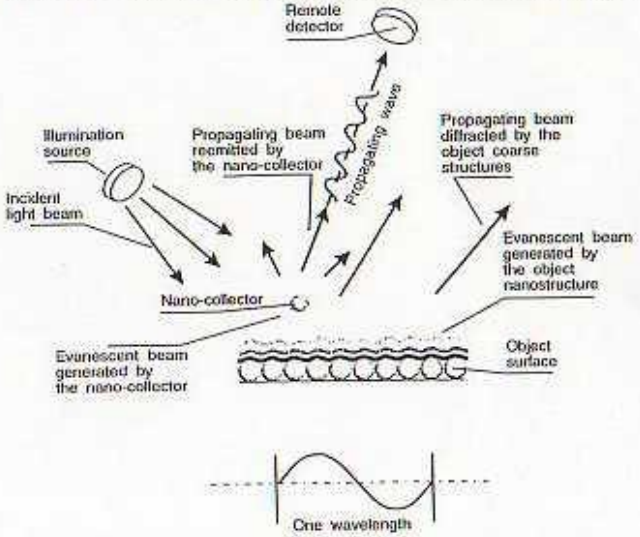

Sketch of near field detection. Step 1: generation of the object near field by the illumination process. A light source illuminates an object represented as composed of discrete components. These components are excited by the incident field and re-emit light. The waves associated to the reflected beam are composed of evanescent waves confined on the object surface and of propagating waves. If the periodic structures of the object are smaller than the wavelength (it is the case of the figure), the reflected field, far away from the object, does not contain any information on the fine structure of the object. Step 2: detection of the near field. For detecting the subwavelength object information, a small scattering centre (the nano-collector) is brought close enough to the object surface. The near field lying on the surface will excite the scattering centre which will re-emit light. The re-emitted light is again composed of evanescent waves (non-detectable) and propagating ones which can propagate far away to the remote detector.

A SPECIAL NEAR FIELD: SURFACE PLASMONS

TWO EXAMPLES

1.

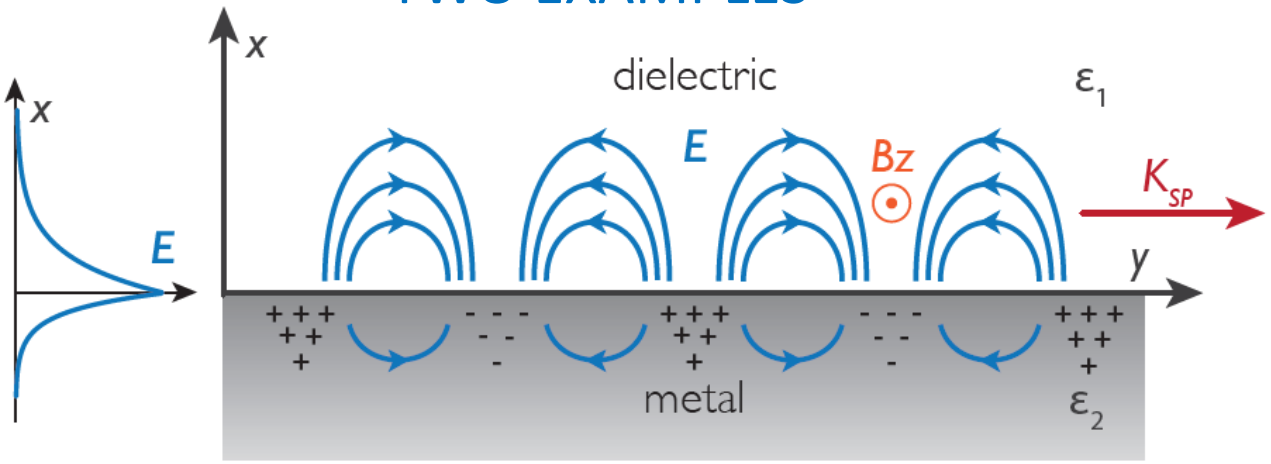

SPP

2.

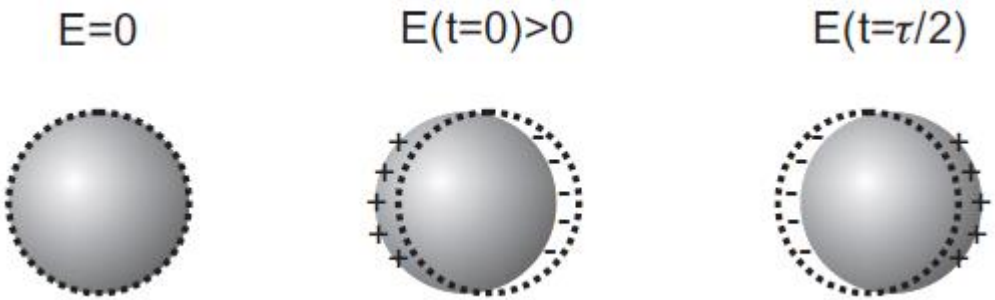

LSPP

Ti:Sa lézer: ʎ=800nm (1.55eV)

1.PROPAGATING SURFACE PLASMONS (SPP)

(EM fields up to 10^{12} W/cm^2)

Surface plasmons dispersion: $k_x = \frac{\omega}{c}\left(\frac{\varepsilon_m \varepsilon_d}{\varepsilon_m + \varepsilon_d}\right)^{1/2}$

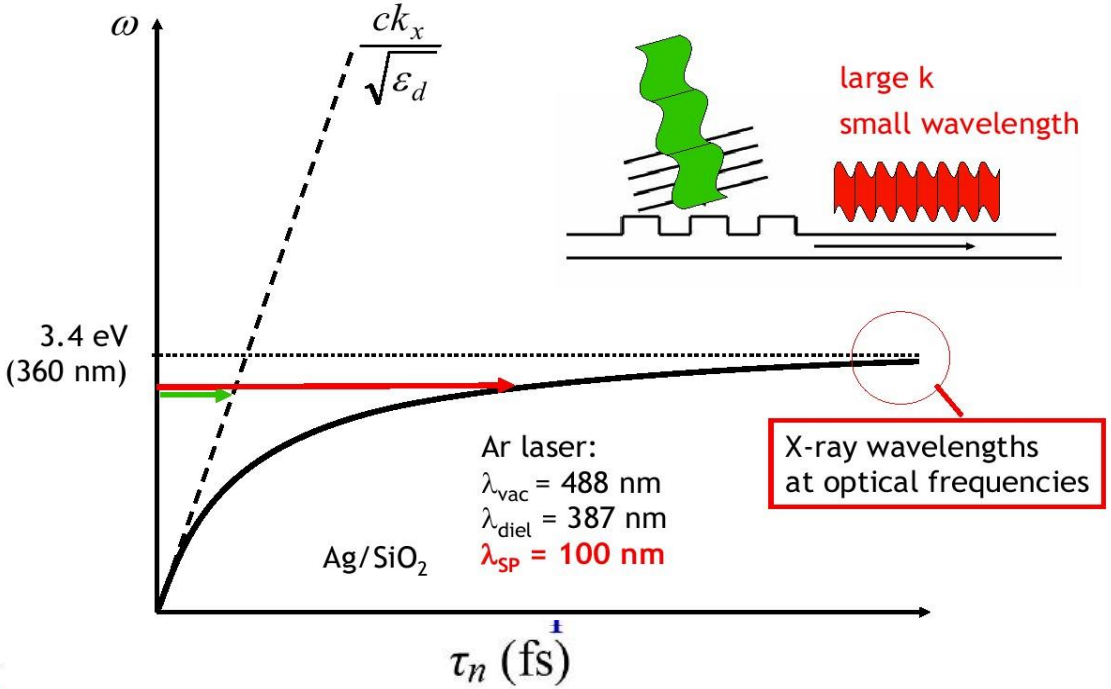

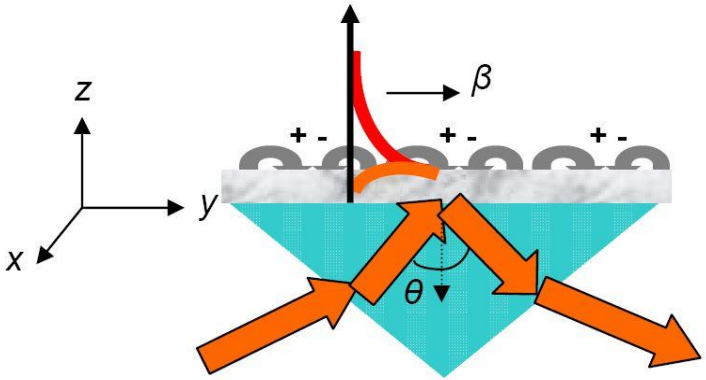

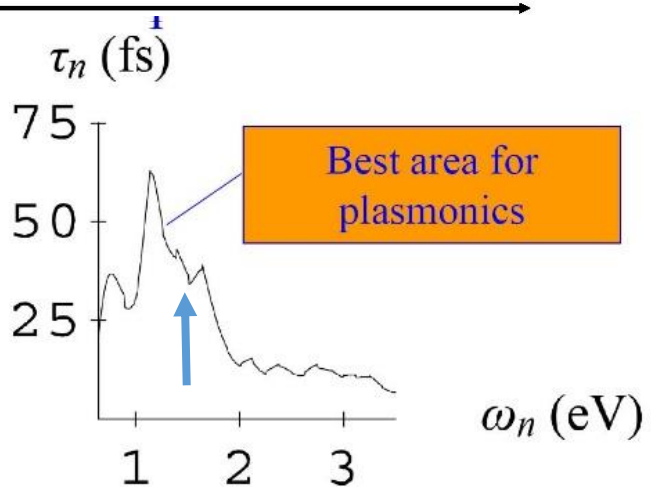

Ti:Sa laser:
pulse length in the
same time domain

NEAR FIELD STM (NO DIFFRACTION LIMIT)

NEAR FIELD:LASER EXCITED SPP-s GIANT EM FIELDS

(Kretschmann geometry)

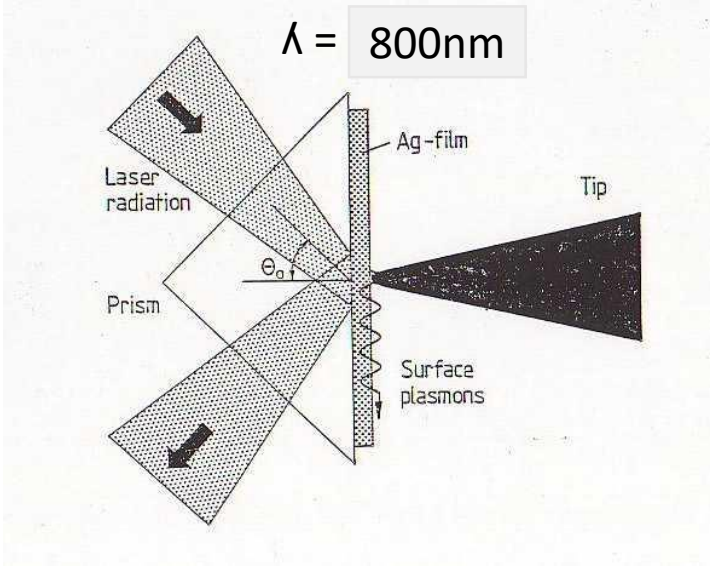

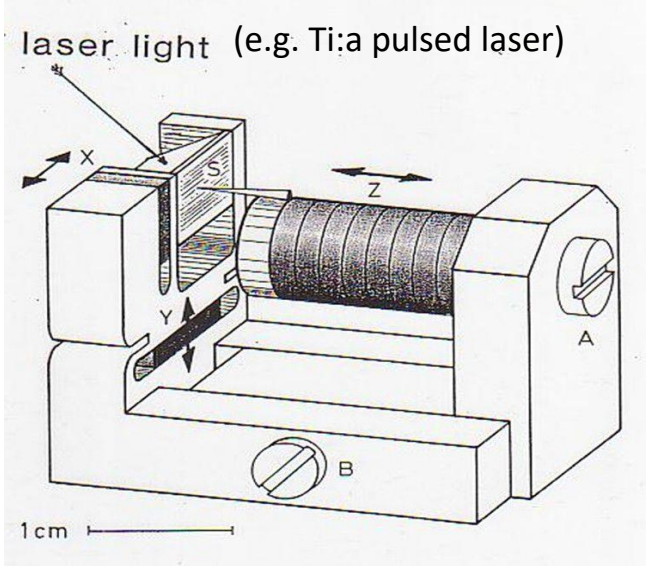

Surface topology 100x100nm Localized SPP field

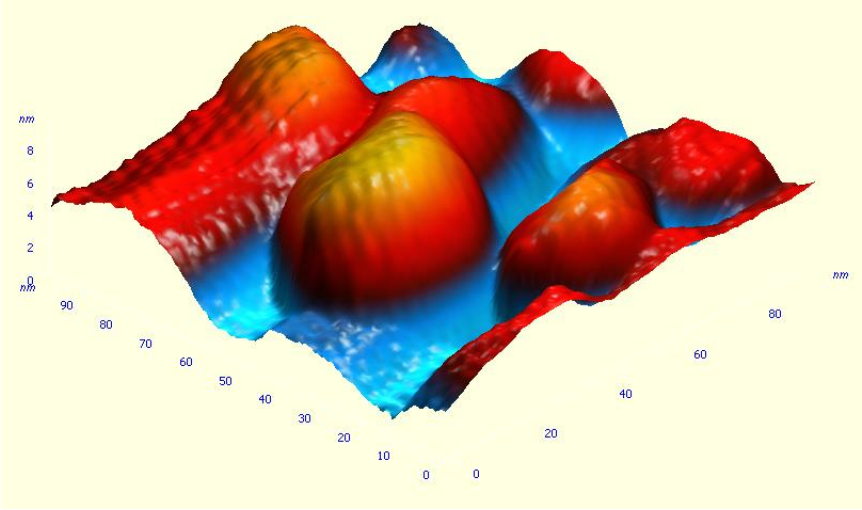

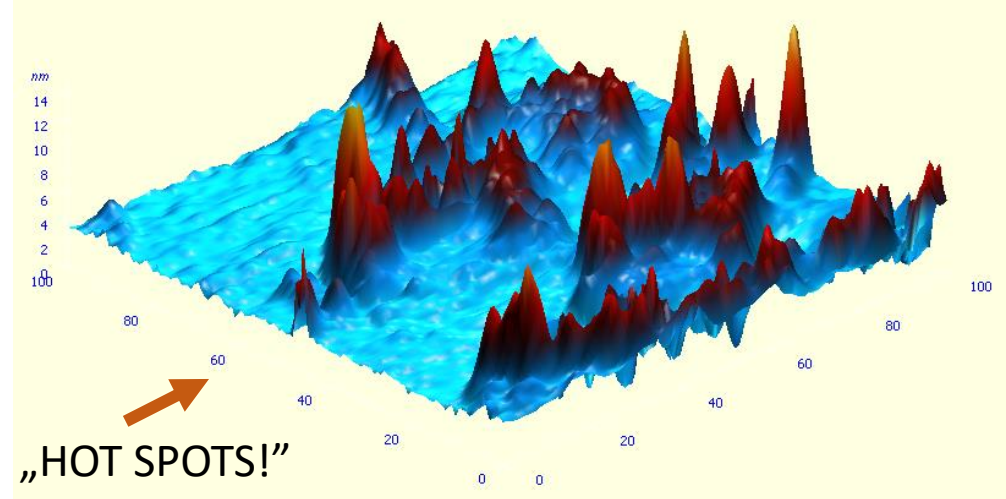

„HOT SPOTS!"

ANOMALY AT ROOM TEMPERATURE!

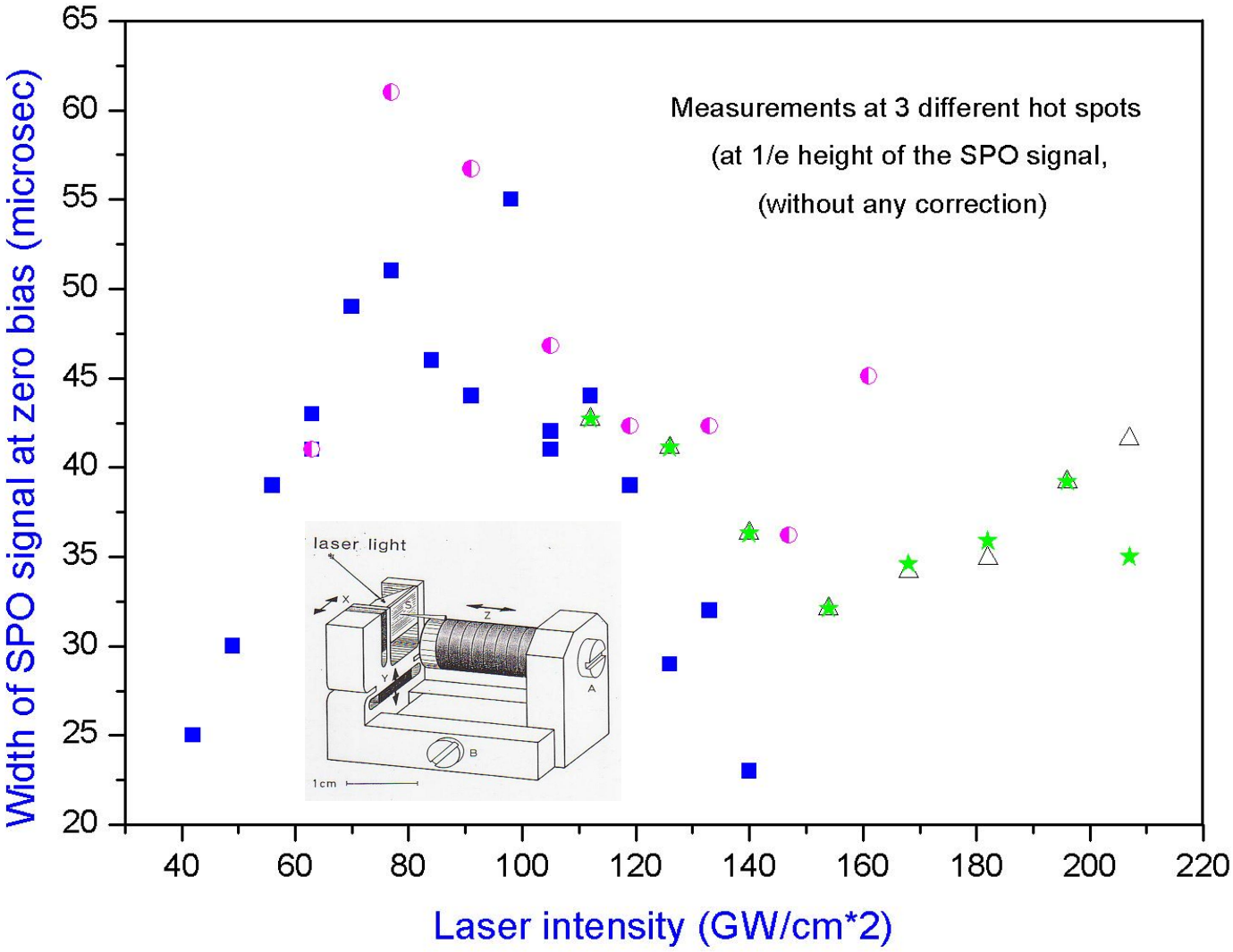

N.Kroo,P.Racz,S.Varro: Nucl Inst Meth Phys B, 369,55 (2016)

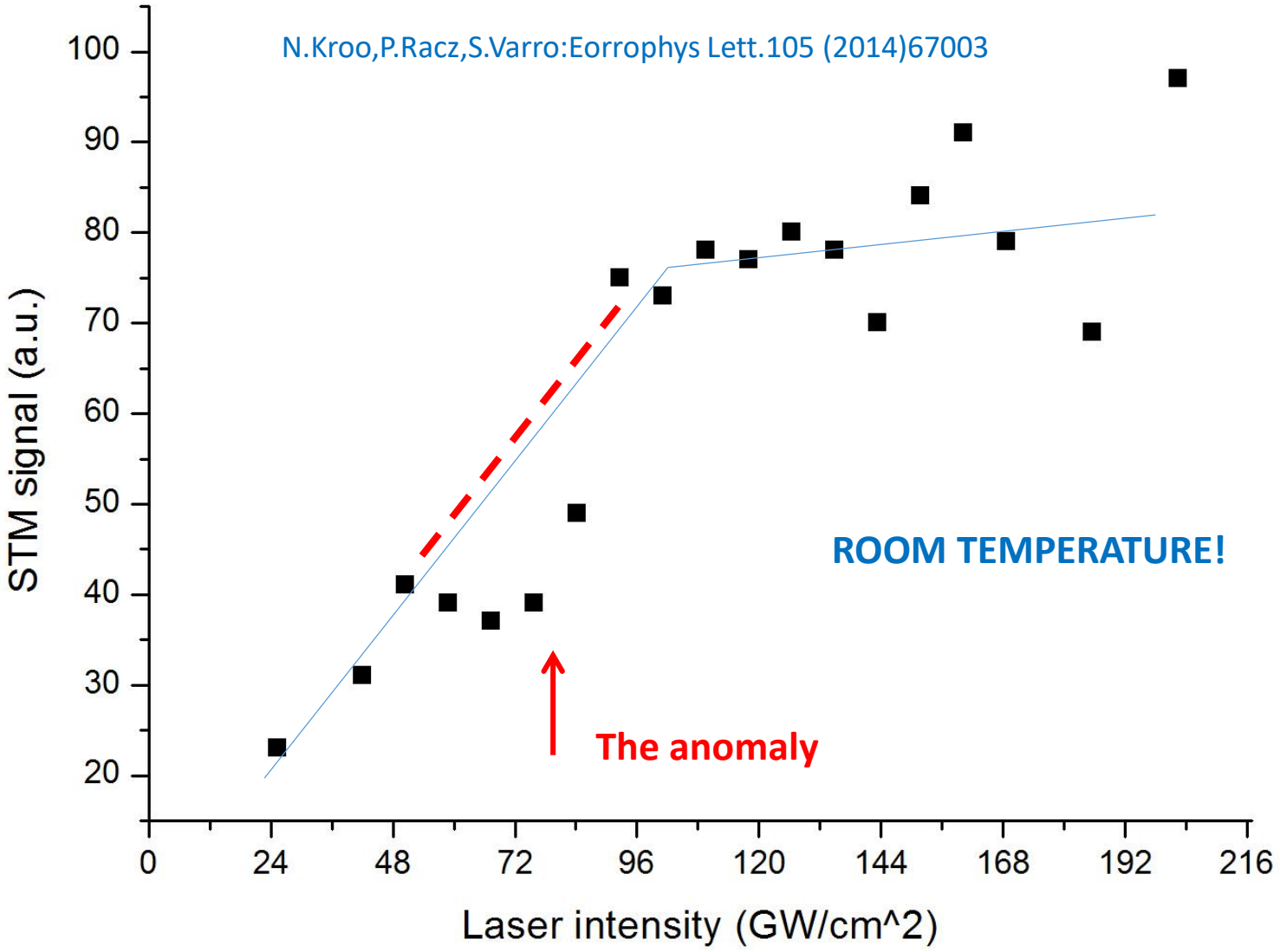
N.Kroo,P.Racz,S.Varro:Eorrophys Lett.105 (2014)67003
STM signal (a.u.)
100
90
80
70
60
50
40
30
20
0
24
48
72
96
120
144
168
192
216
Laser intensity (GW/cm^2)
ROOM TEMPERATURE!
The anomaly

ELECTRON-ELECTRON INTERACTION: THE EFFECTIVE POTENTIAL IN STRONG EM FIELDS

$$V_{eff}(\boldsymbol{r}) = V(\boldsymbol{r}) J_n[z_1 \sin(\boldsymbol{k}\cdot\boldsymbol{r}/2)]$$

$$z_1 = 2\mu(c\Delta p'_\perp / \hbar\omega)$$

$$\mu = eF / mc\omega$$

$$V(\boldsymbol{r}) = e^2 / r$$

F: The amplitude of the EM field

Plasmon field amplification: ~40

Electron pairing!

If the effective potential is negative!

J.BERGOU,S.VARRO, M.V. FEDOROV:1981

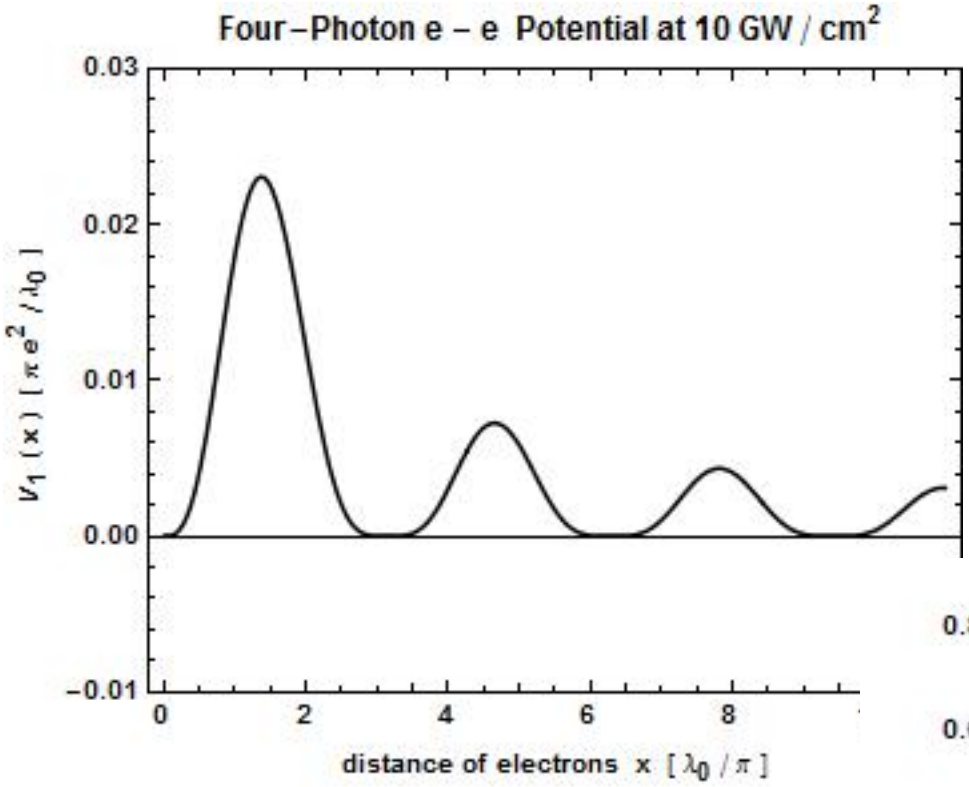

THE EFFECTIVE POTENTIAL FOR 2 LASER INTENSITIES (including the field amplification of the SPP-s)

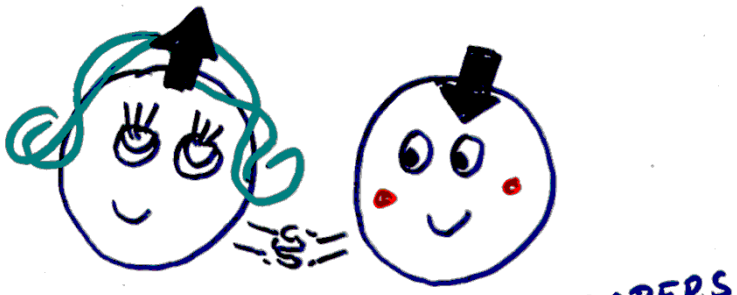

Kis távolság

THE COOPERS

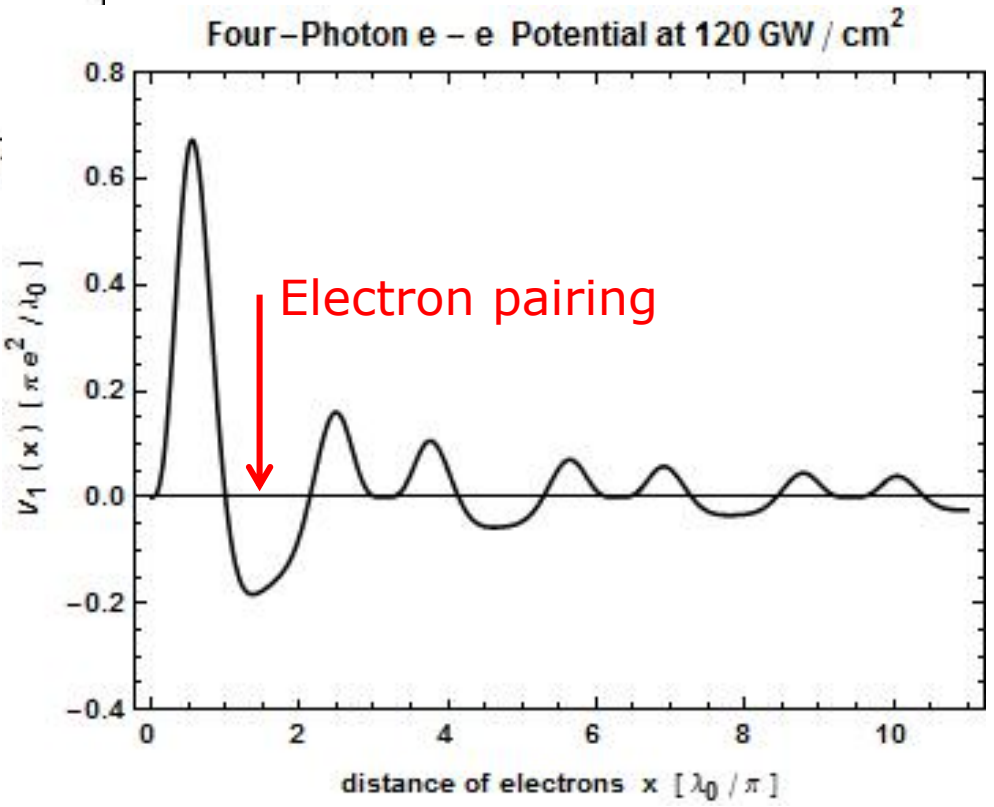

Matter under extreme conditions (extremely high intensities)

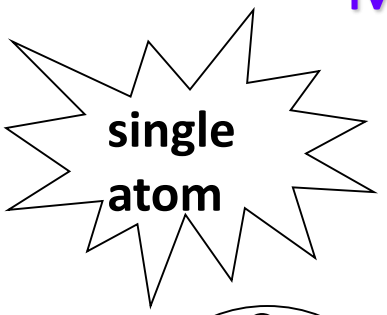

$I = 10^{16}$ W cm^{-2} → E ~ 10^{9} V/cm

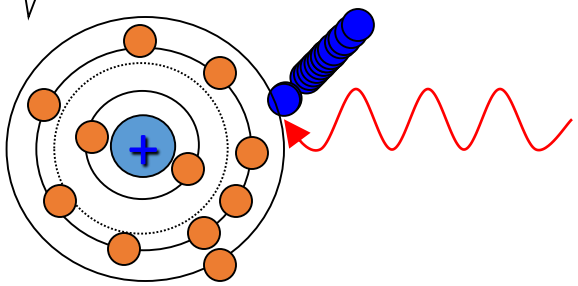

High intensity
Photoeletric Effect

Rapid ionization of valence electrons

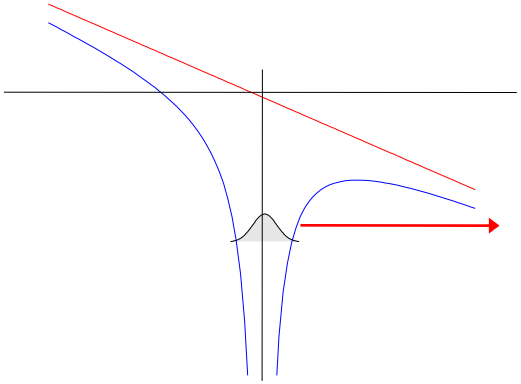

$$V = -\frac{q}{x} \pm E.x$$

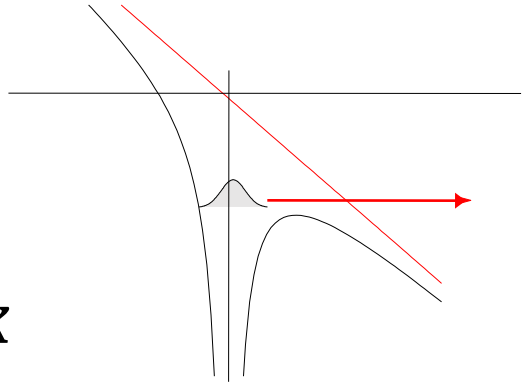

Tunnelling

10^{14} - 10^{15} W cm^{-2}

Over the barrier

> 10^{15} W cm^{-2}

Each atom loses at least one electron. Some can lose as many as 6 !

MULTIPHOTON ELECTRON EMISSION FROM GOLD

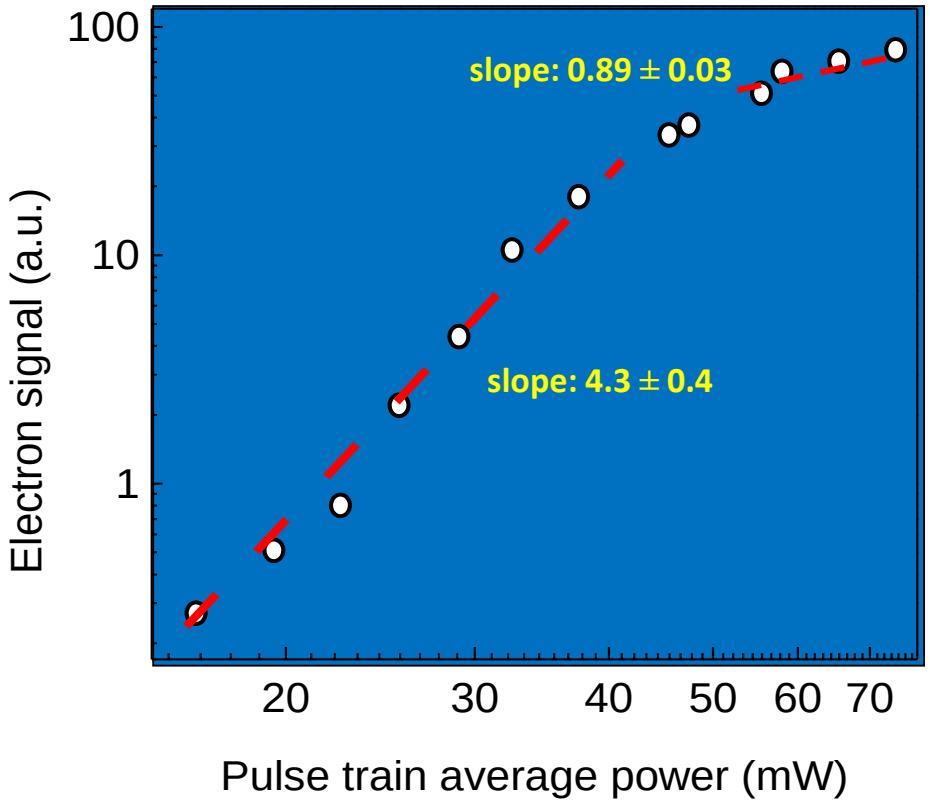

PLASMONIC ENHANCEMENT!

Multiphoton ⟹ tunneling transition at ~4×10^{10} W/cm^2 incident intensity, ~5.5×10^8 V/m field

Keldysh-gamma γ=31

→ indication of well-known field enhancement of surface plasmonic fields

$$\gamma^2 = \frac{W}{2U_p} = \left(\frac{\omega\sqrt{2mW}}{eE_l} \right)^2$$

W: work function, E_l: laser field strength

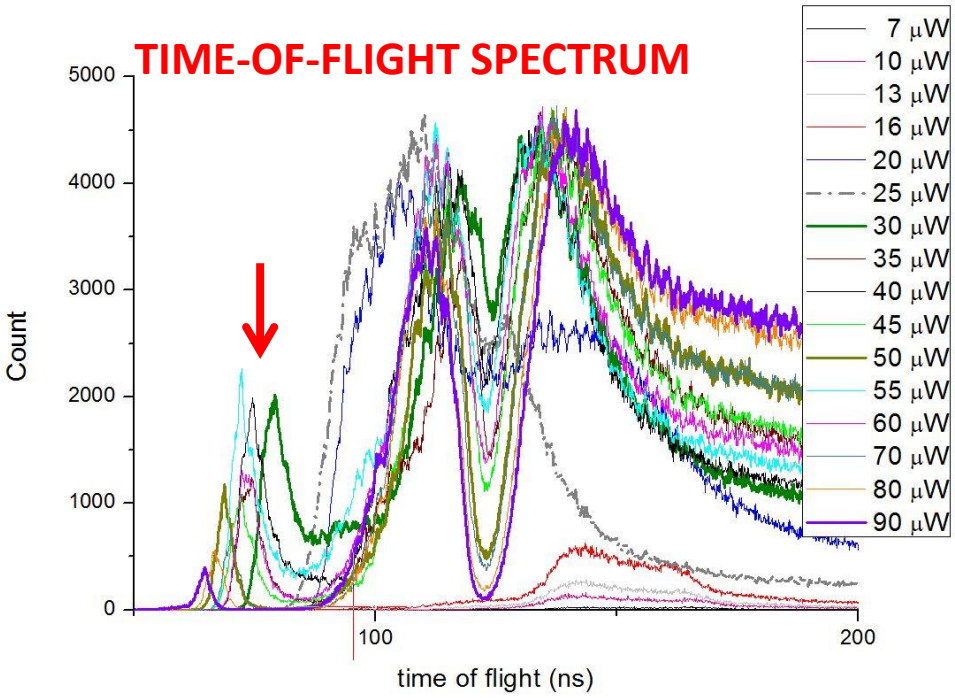

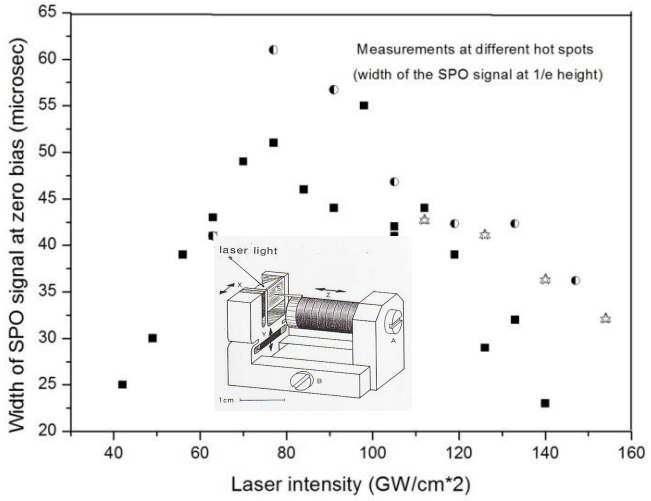

Multiplasmon electron emission

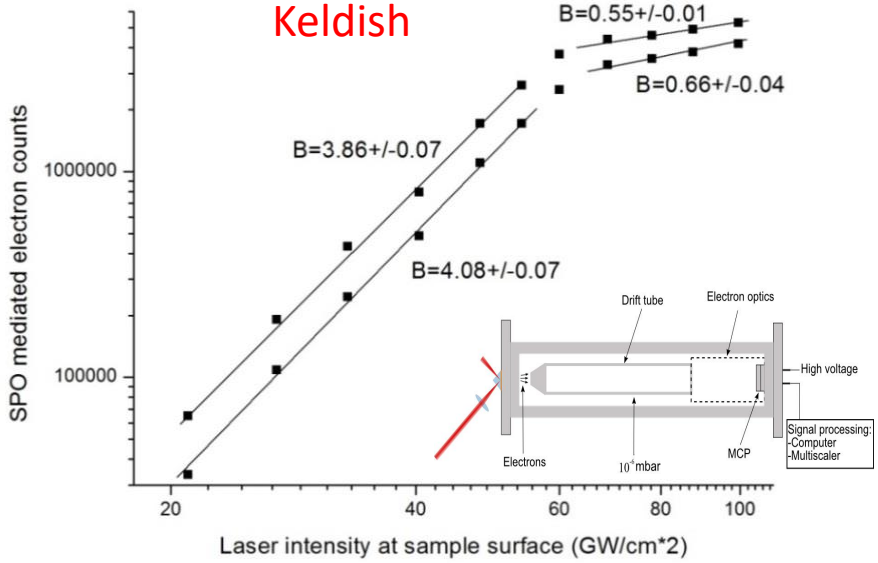

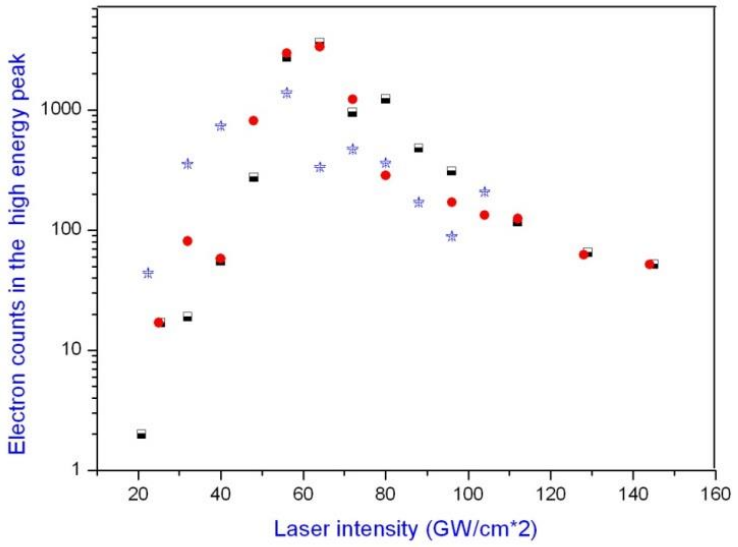

N.Kroo,P.Racz,S.Varro: EPL 105,67003 (2014)

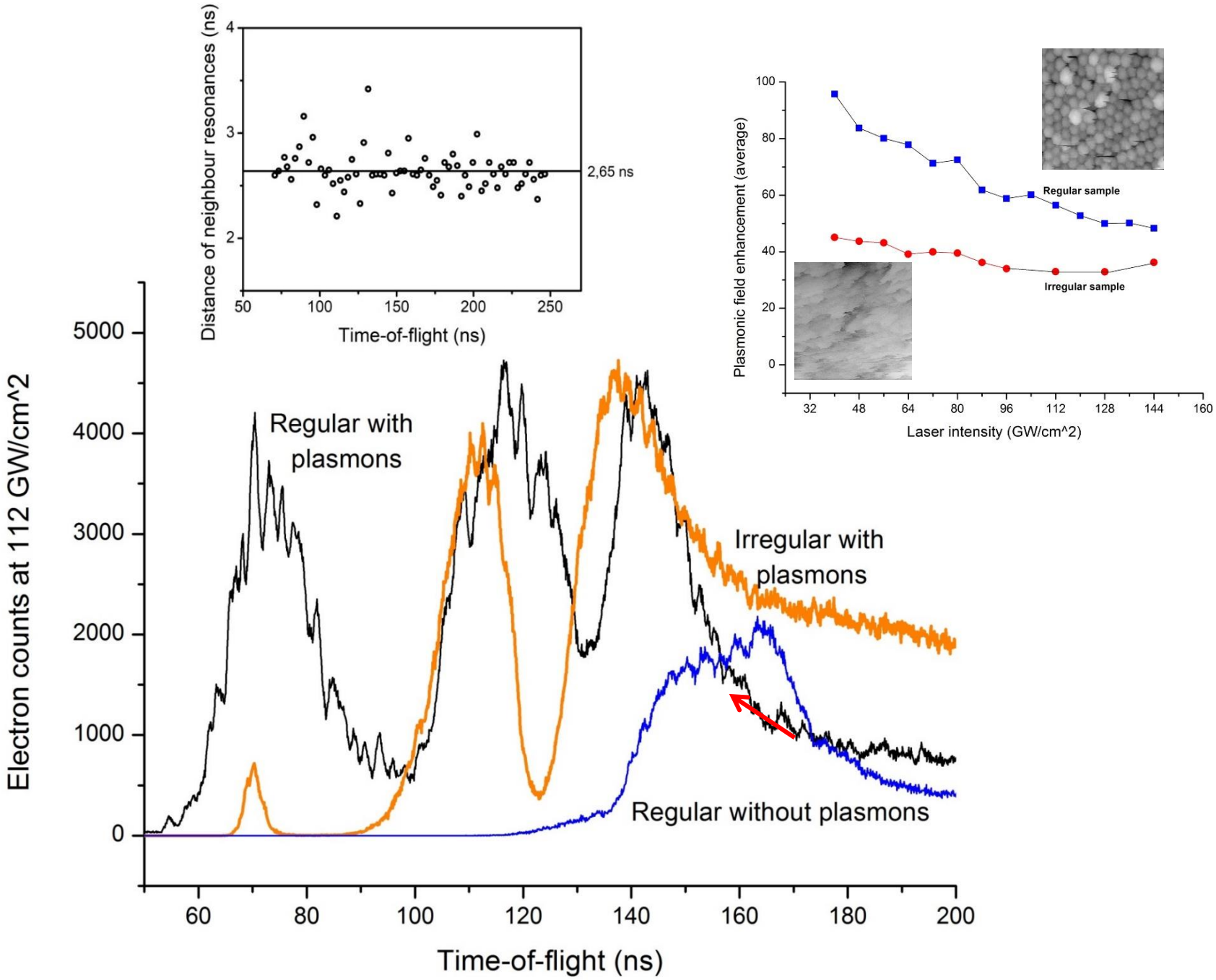

20160831,20130926,20170412

MAGNETIC (RECTIFIED EM) FIELD DEPENDENCE
(Meissner effect)

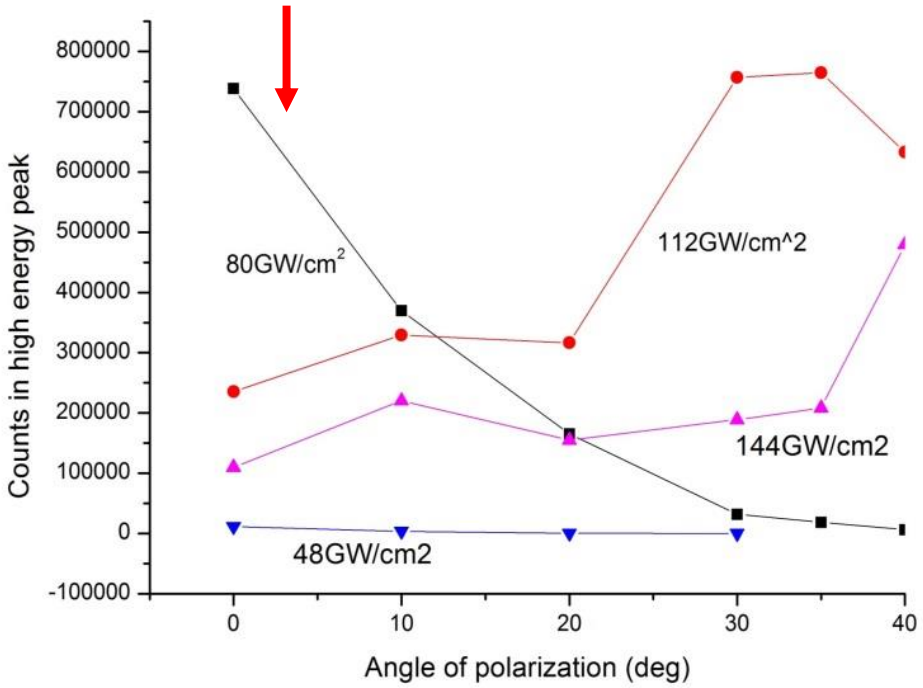

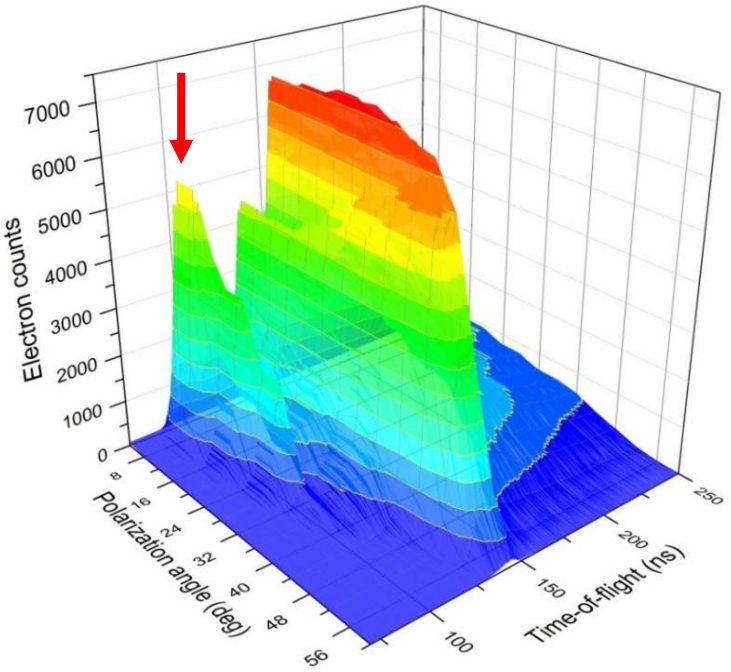

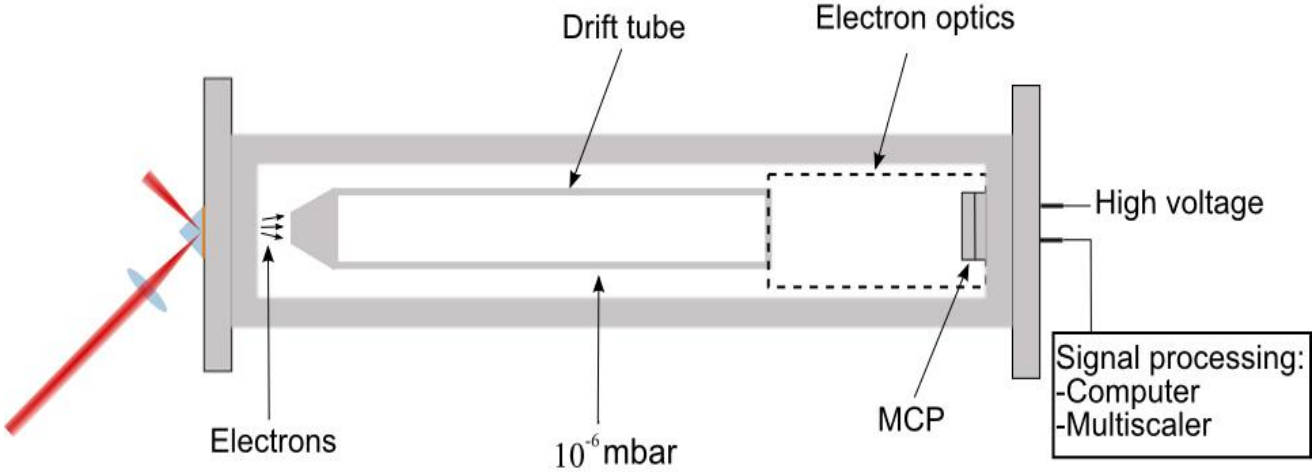

P.Racz, N.Kroo: Phys Wave Phen 27(3)192(2019)

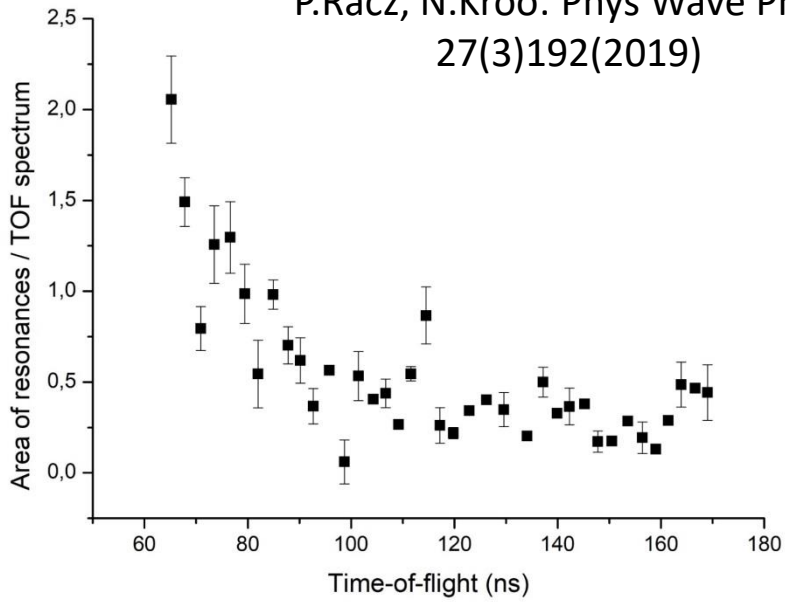

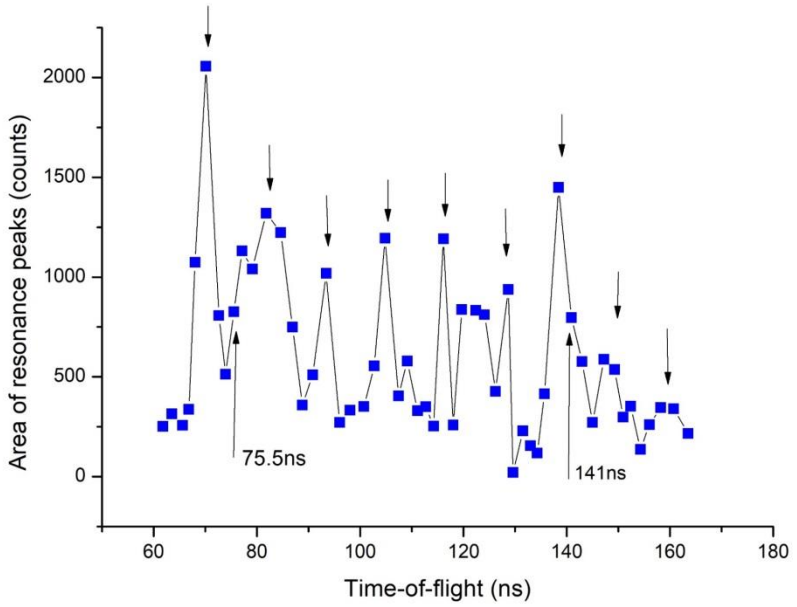

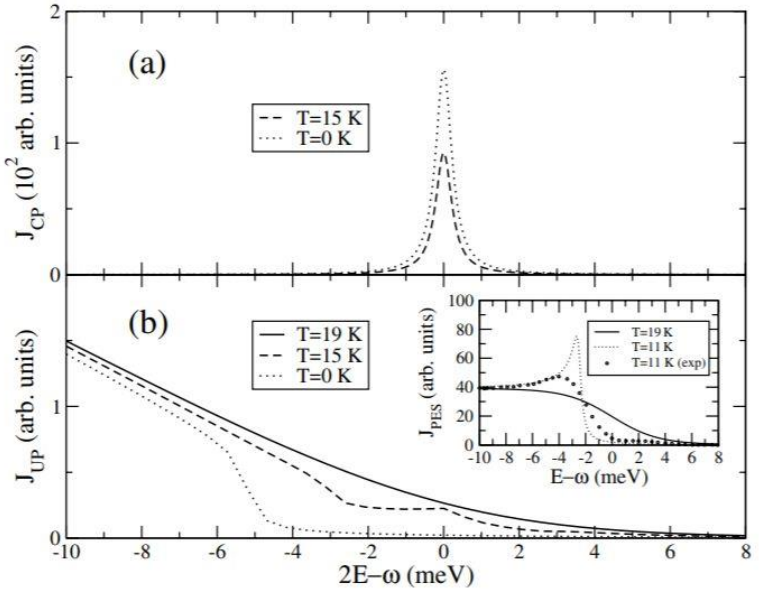

FIG. 2. DPE current from V_3Si ($\Delta_0 = 2.6\ meV$, $T_c = 17$ K) as a function of the energy $2E - \omega = E_{12}$ and temperature. Panels (a) and (b) show J_{CP} [Eq. (10)] and J_{UP} [Eq. (9)]. Theoretical results and experimental data [15] for the angle-integrated single photoemission are included in the (b) inset.

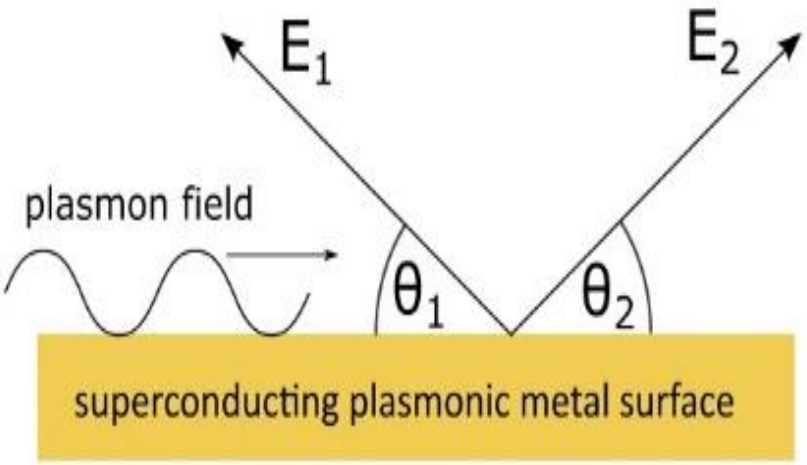

CONCLUSIONS 1

a.„SMOOTH" SAMPLE

Electron pairing and ideal diamagnetism

b.STRUCTURED SAMPLE

Electron pairing confirmed. Significantly enhanced effect.

Increased SPP field amplification.

A sequence of equidistant narrow resonances in the total TOF spectrum, but different parameters (EM field dependence of the width and area) in the high energy peak then in the remaining part of the spectrum.

Slower decay of the resonance areas!

Fast processes streched out in the TOF spectrum (~10^6 times)

Less frequent extra high intensity resonances in the electron pairing laser intensity range: coincident detection of the Cooper electron pairs

2.LOCALIZED PLASMONS (LSPP) UP TO 10^{20} W/cm^2)

(The basic difference between SPP-s and LSPP-s)

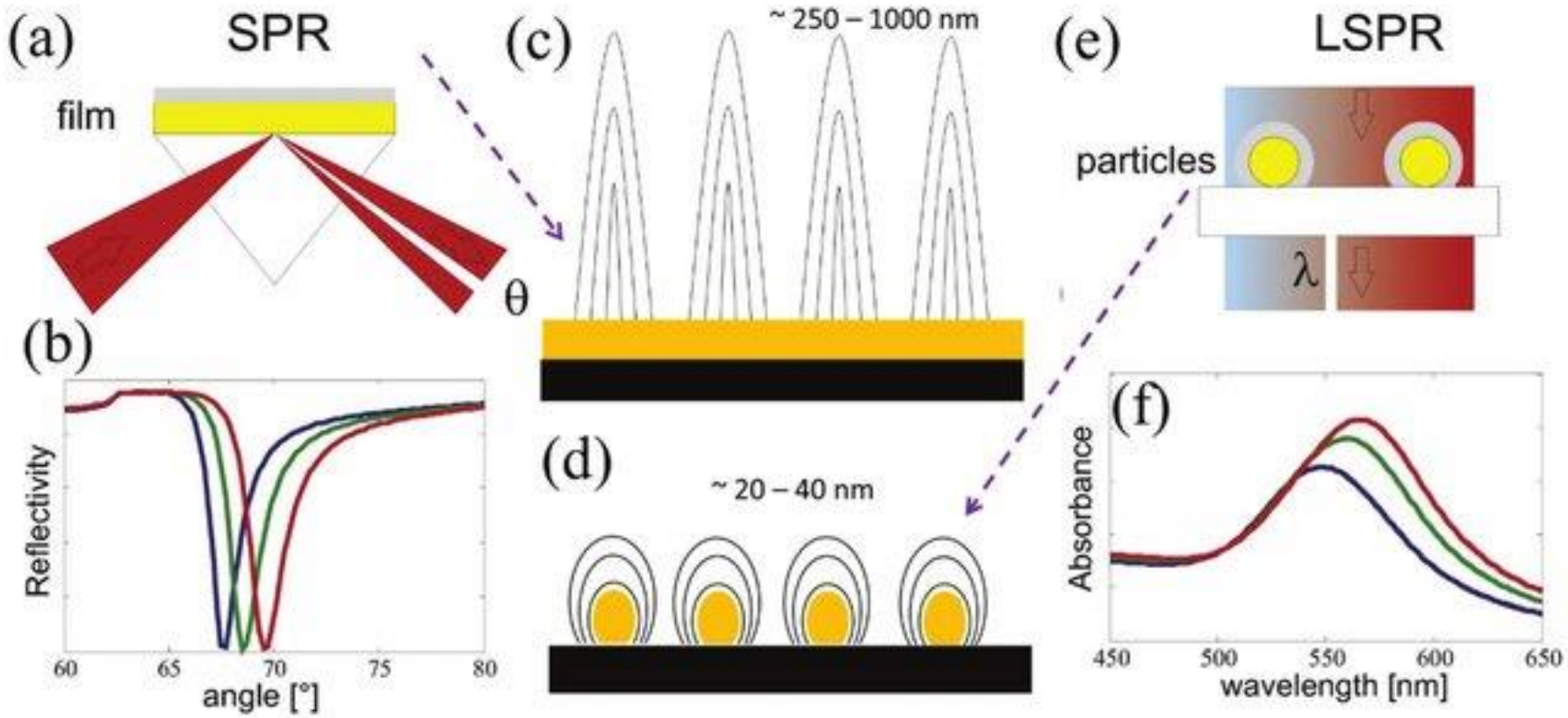

LSPP: -NO PENETRATION INTO THE PLASMONIC MATERIAL (e.g. metal)

- SMALLER PENETRATION INTO THE DIELECTRIC /VACUUM
- NO DISPERSION
- BROADER RESONANCE

LIGHT PENETRATION INTO THE TARGET

Plasma absorption

- A = 1-R

$I < 3 \times 10^{13}$ W cm^{-2}, A is almost polarization independent & obeys Fresnel laws, as IB is dominant

- at higher intensities, there is a clear polarization dependence of absorption

- the difference in absorption should account for extra absorption mechanisms, which are polarization dependent

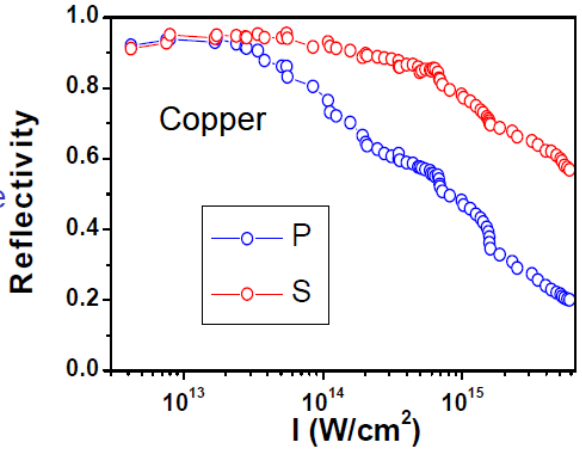

R vs I at 45°

TIFR data

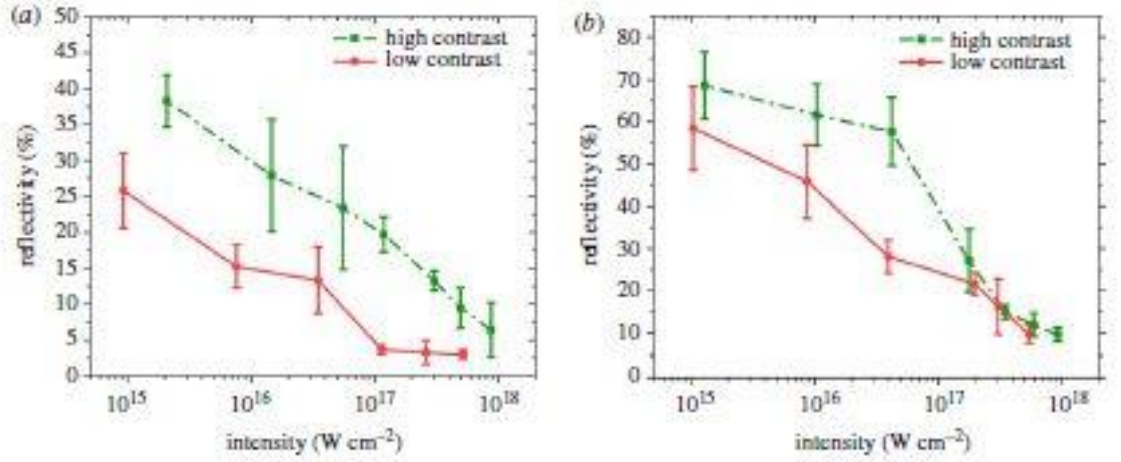

Figure 2. Measured reflectivity from (*a*) gold and (*b*) boron targets. The red circles (solid line) correspond to the case of low and the green squares (dotted line) the high-contrast case.

Zs.Kovács, I.B.Földes: Phyl.Trans.R.Soc A378 20200043 (2020)

LSPP EFFECT: HIGHER SPOTS AT LOWER FIELDS (up to 10^{15} W/cm^2)

Laser pulse energy dependent spot size

Non Au nanoparticle doped polymer

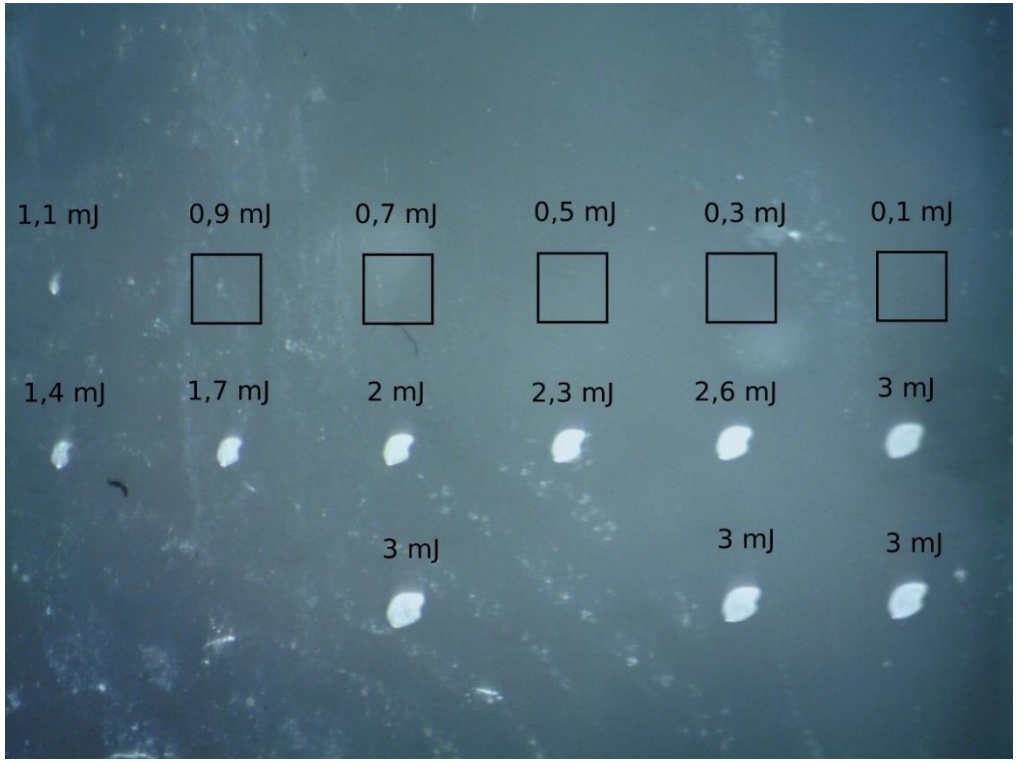

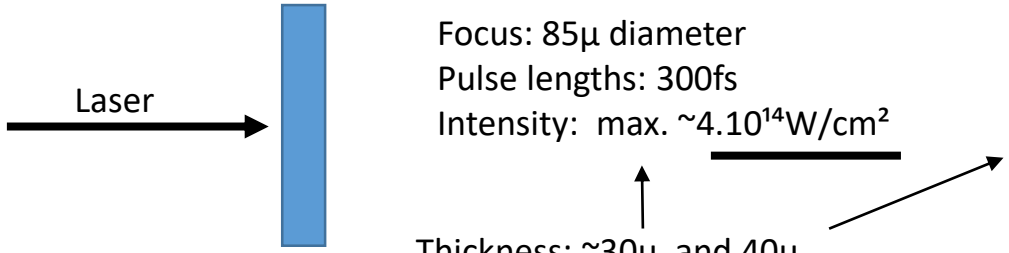

Doped polymer

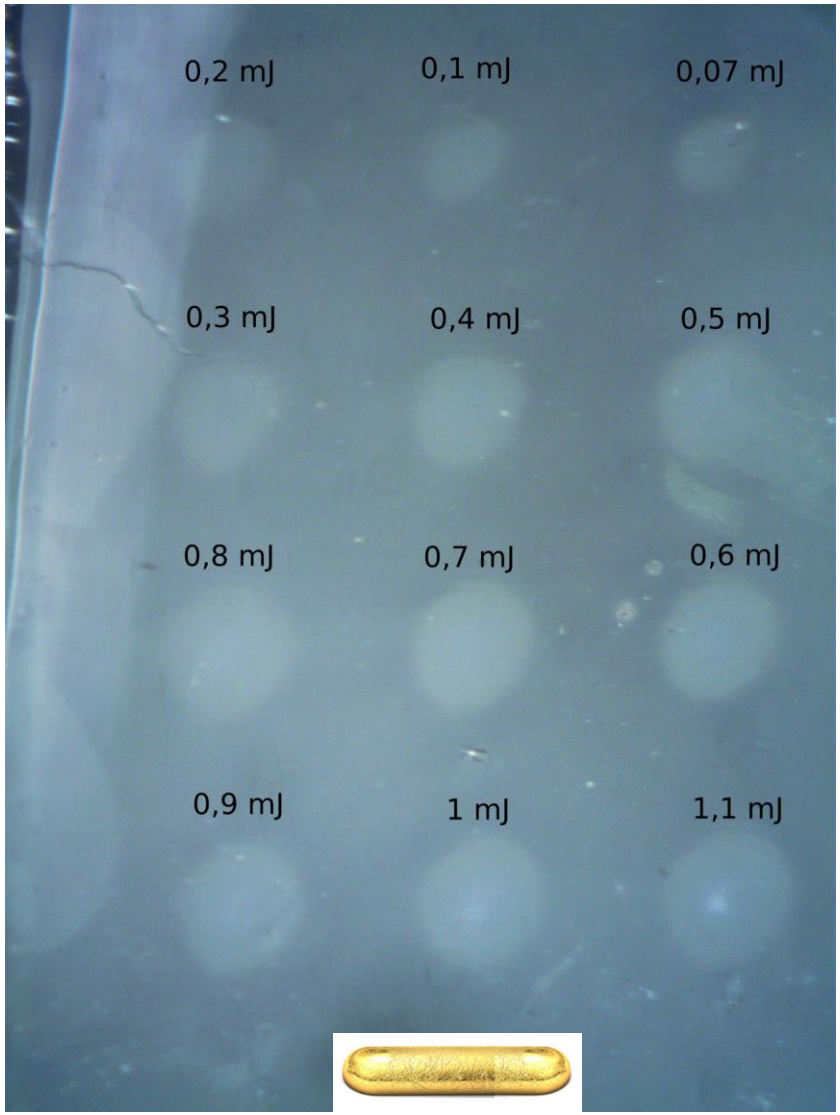

A few per mill resonant gold nanoparticles arany

Laser pulse length: 300 fs

Ti:Sa laser: ʎ=800nm, ~1.55eV

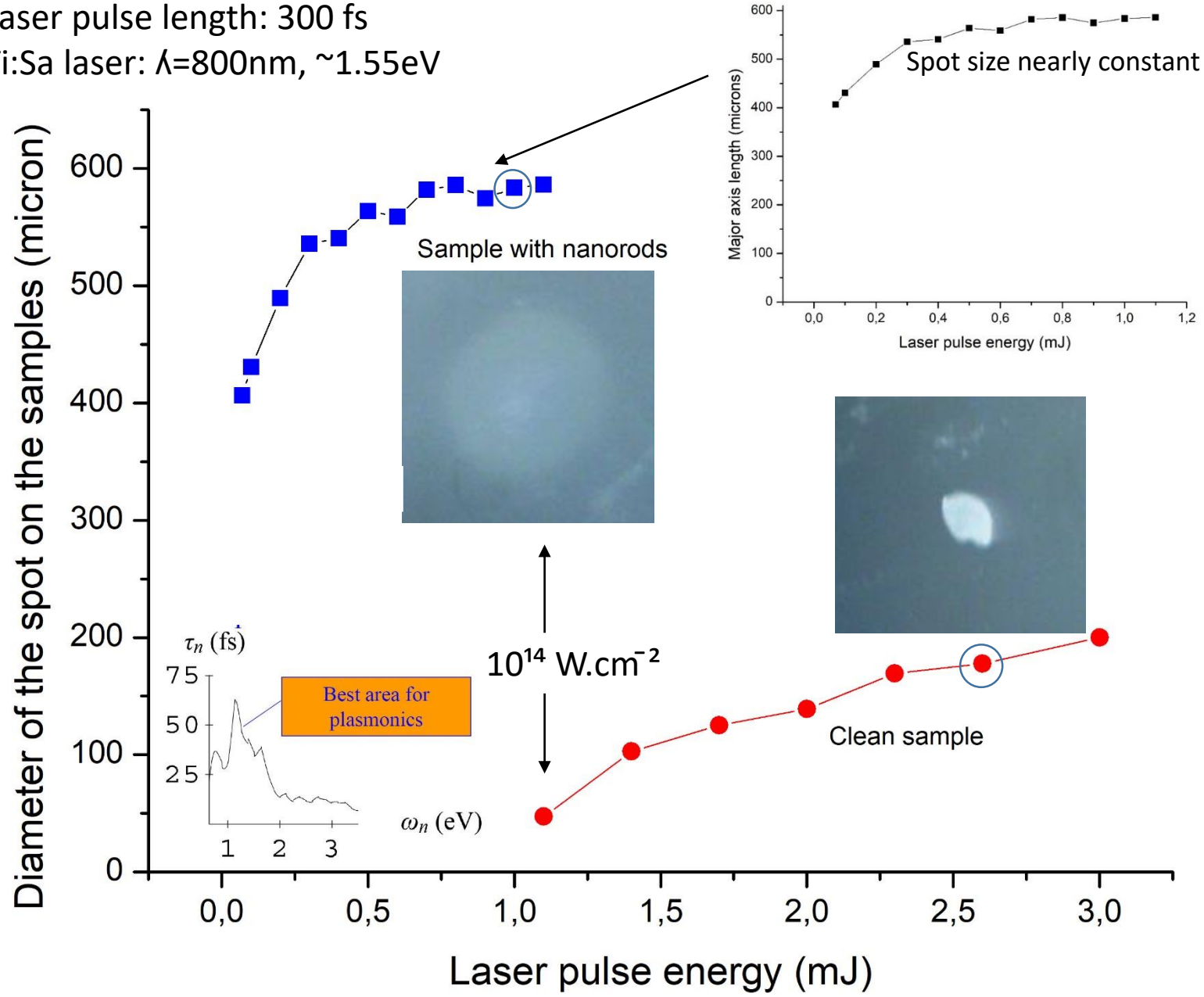

Giant plasmonic amplification; the laserlight reaches the nanoantennas;

AND UP TO ~10²⁰ W/cm²

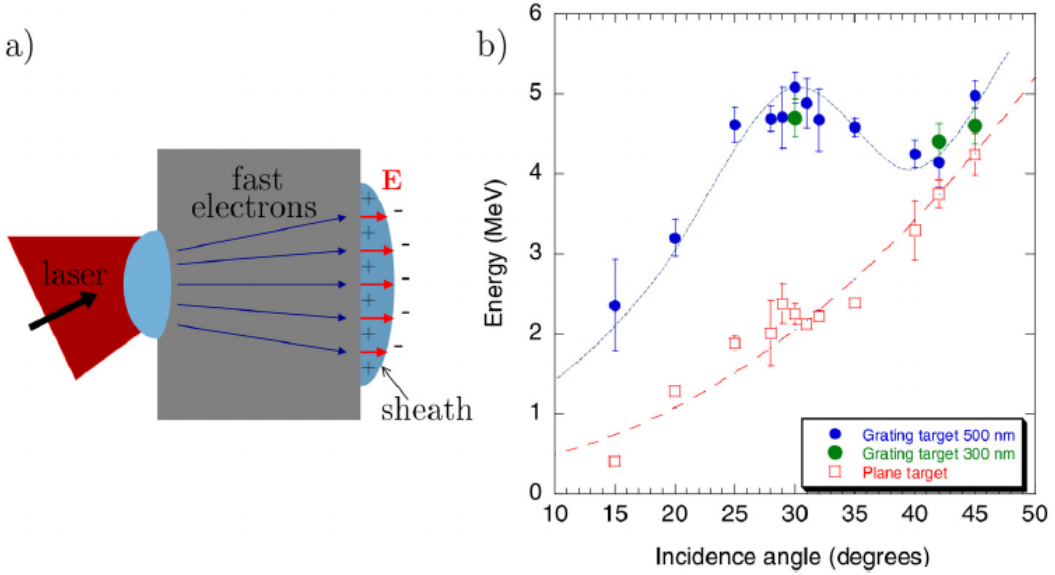

FIG. 5. Plasmon-enhanced TNSA of protons.[95] (a) Schematic of TNSA. The fast electrons produced by the interaction at the front side cross the target and produce a sheath at the rear side, where ions are accelerated. (b) Experimental data from the interactions of a high-contrast 25 fs, 2.5×10^{19} W cm^{-2} laser pulse with solid plastic targets. The cut-off energy of protons emitted from the rear measured as a function of the incidence angle from both flat and grating targets (for two different values of the grating depth). An up to 2.5-fold energy increase is observed for gratings, with a broad maximum around the resonant angle for SP excitation (30°). Data from Ref. 95.

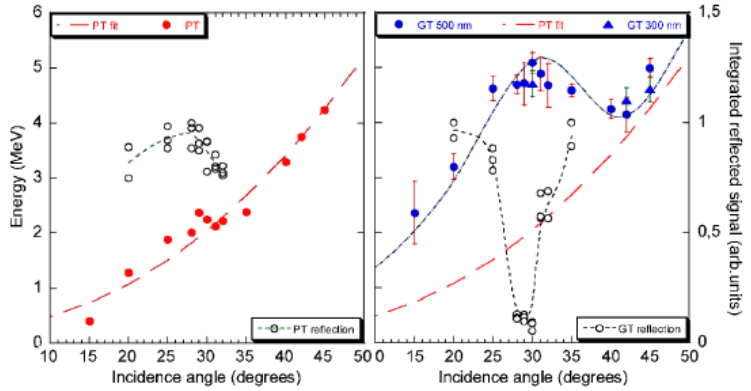

FIG. 3 (color online). Maximum proton energy (filled data points) and reflected light signal (empty data points) as a function of incidence angle α. Left and right frames correspond to 20 μm thick plane targets and to 23 μm thick grating targets, respectively. Filled circles and triangles correspond to 0.5 and 0.3 μm deep gratings, respectively. The (red) dashed line is proportional to $\sin^2\alpha/\cos\alpha$. The other lines are guides for the eye.

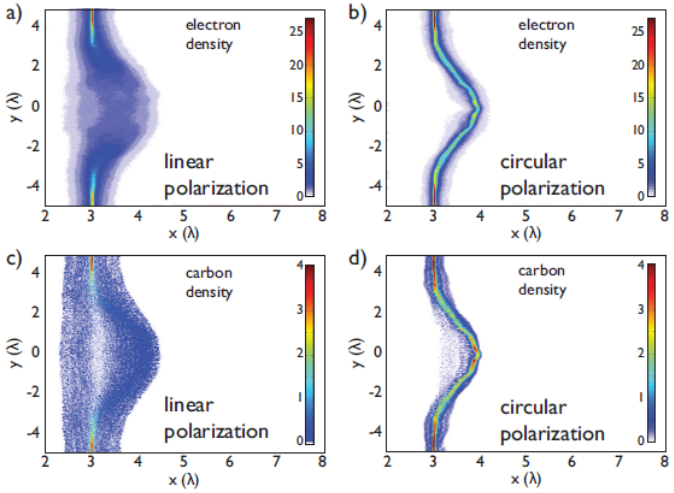

FIG. 4: (color). Cycle-averaged electron (a,b) and carbon ion (c,d) density at $t = 61$ fs after the peak of the laser pulse reached the 5.3 nm target initially located at $x = 3\lambda$. While linear polarization results in strong expansion of the target caused by hot electrons, for circularly polarized irradiation the foil is accelerated as a dense, quasi-neutral plasma bunch.

OUR PROPOSAL:

NANOSHELL
(nx10nm)

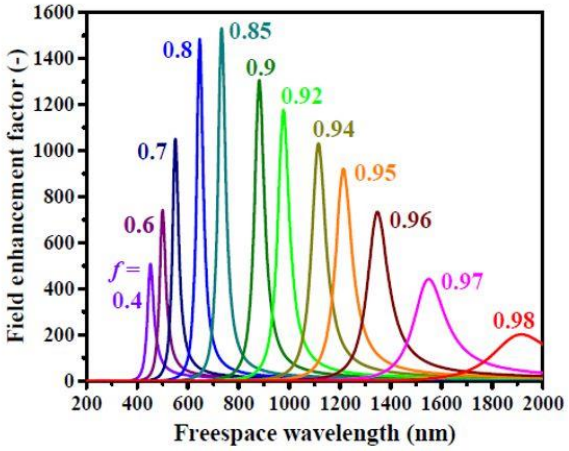

λ = 800nm

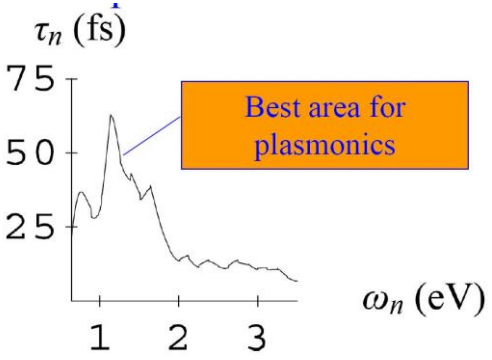

NANOROD (~85x25nm)

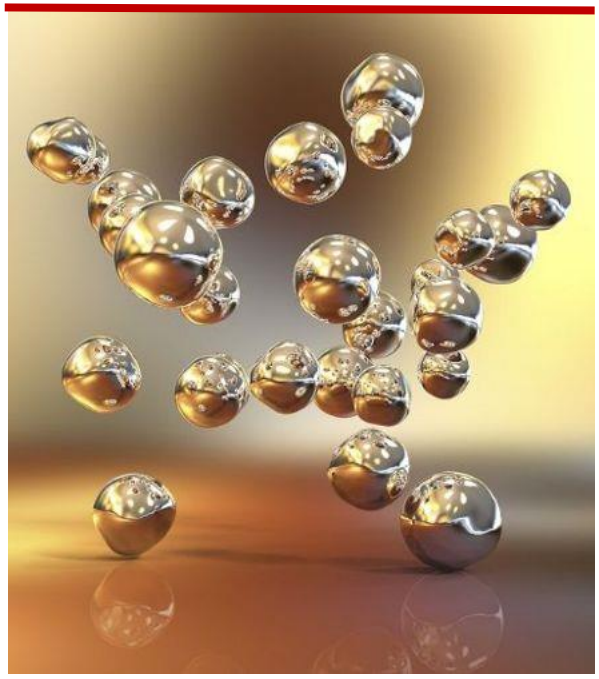

n.10μ

NANOPARTICLES IN
THE FUSION MATERIAL

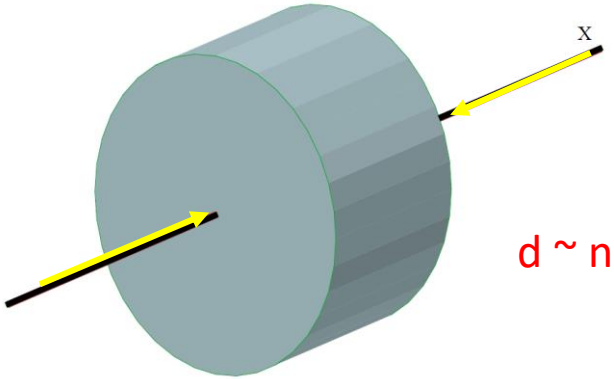

d ~ n.10μ

FEMTOSECOND LASER PULSES
HIGH REPETITION FREQUENCY
LIGHT SPEED: NO TIME FOR INSTABILITIES,ONLY TWO BEAMS, VOLUME IGNITION

Here only indications. Details by L.Csernai (theory), P.Rácz, A.Bonyár and M.Veres (experiments)

DIAGNOSIS No1

SEM IMAGE OF UDMA WITH AU NANORODS

SEM IMAGE OF UDMA WITHOUT AU NANORODS

And Zygo images of the craters

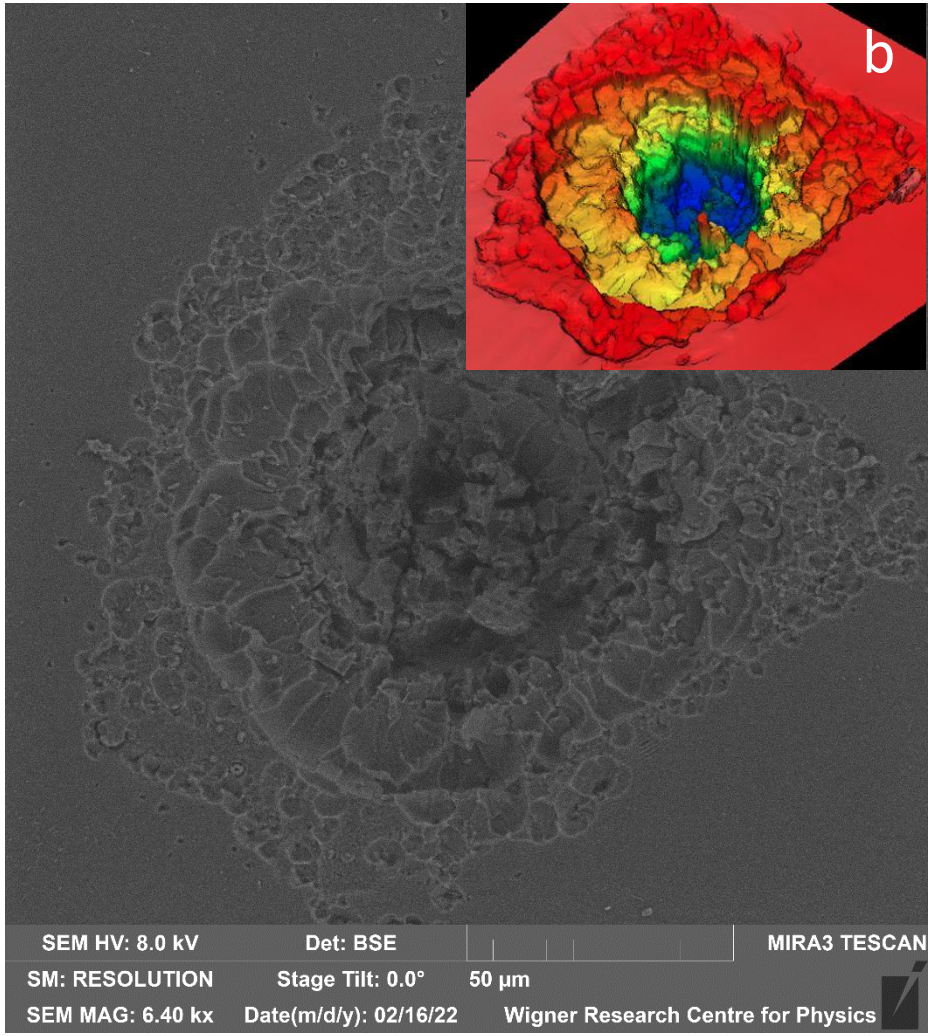

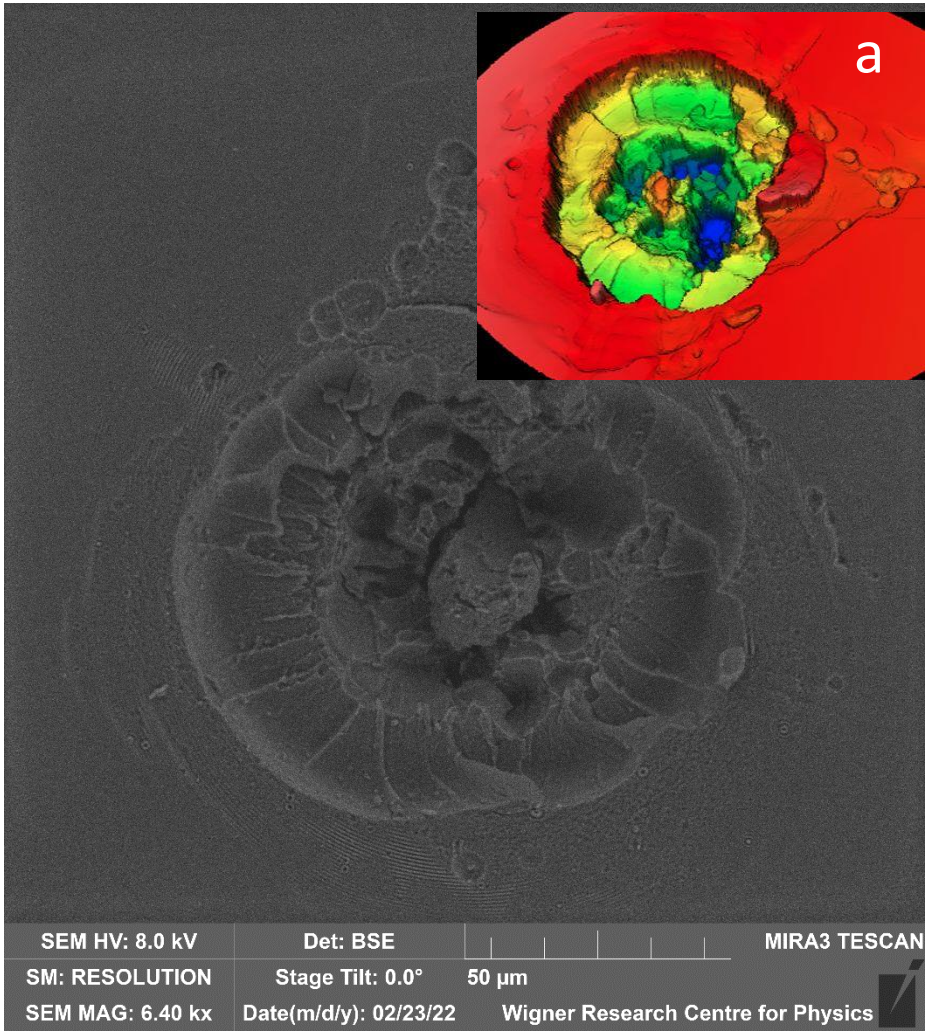

Images at 17.5mJ laser energy, $1{,}16.10^{17}$ W/cm² laser intensity.The volume of the crater of the sample with nanorods (b) is 1.98 times that of the sample without rods (a).

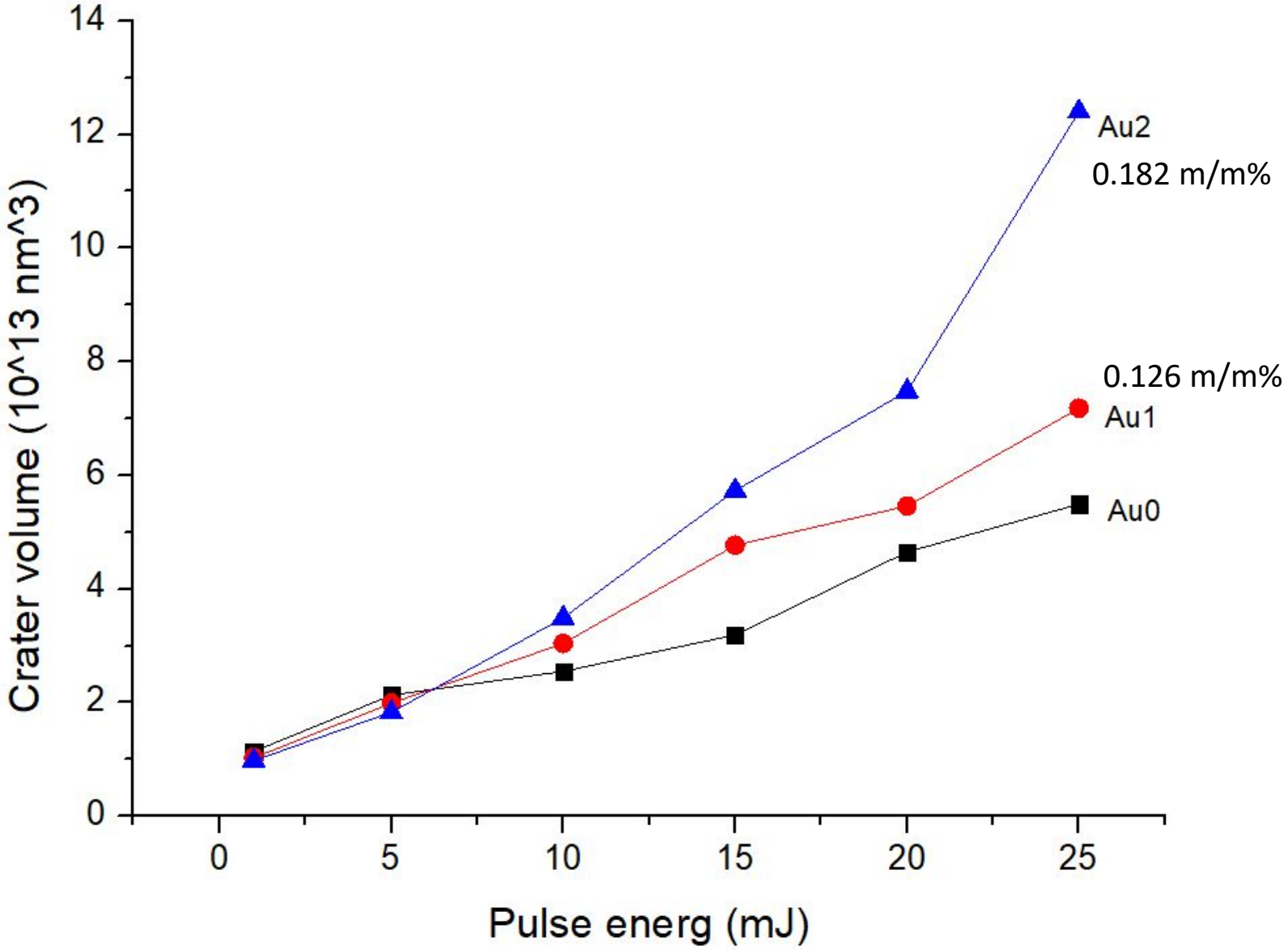
Crater volume (10^13 nm^3)
Pulse energ (mJ)
0
2
4
6
8
10
12
14
0
5
10
15
20
25
Au2
0.182 m/m%
0.126 m/m%
Au1
Au0

DIAGNOSIS METHOD No2 :Raman scattering from the crater surface

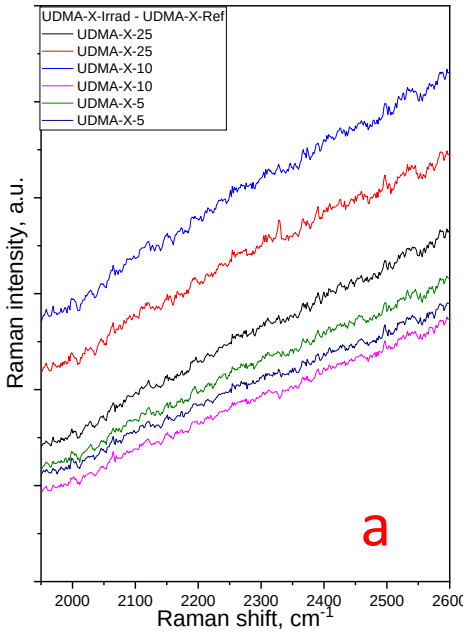

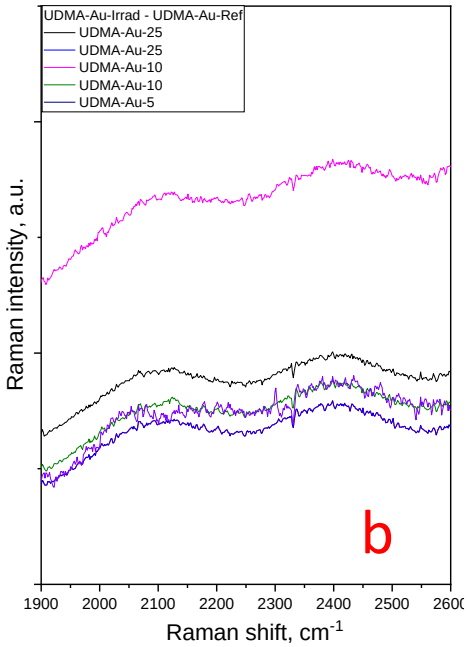

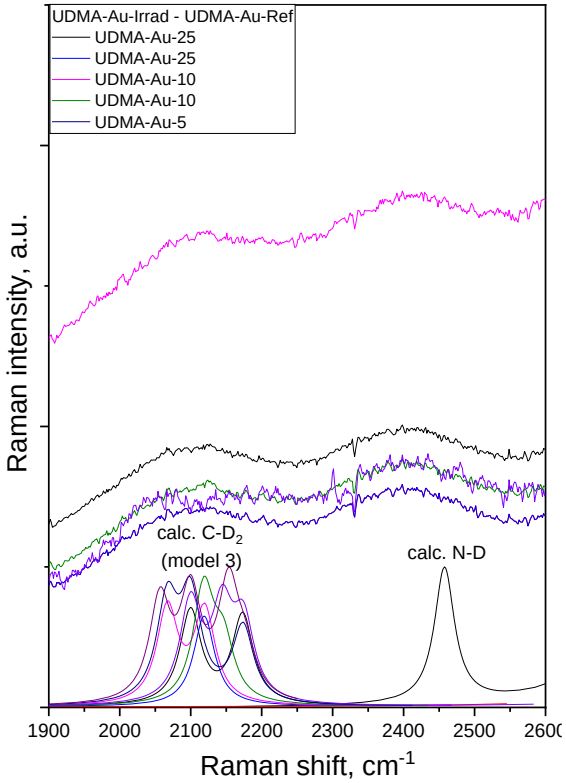

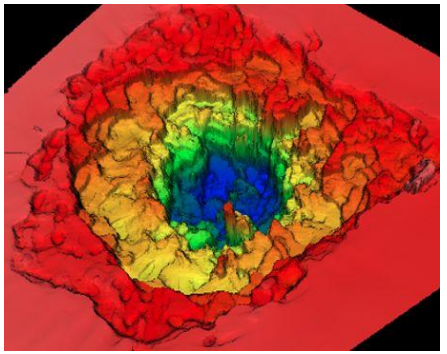

$I_{laser} > 10^{16}$ W/cm²

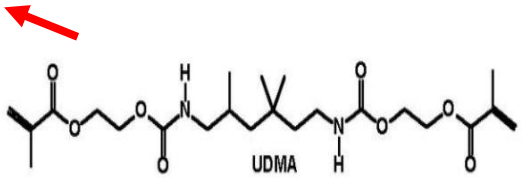

	Peak 1			Peak 2		
Sample	Pos., cm^{-1}	FWHM, cm^{-1}	A, a.u.	Pos., cm^{-1}	FWHM, cm^{-1}	A, a.u.
UDMA_ref	2083	74,01	0,58	2283	98,82	1,03
UDMA_17,5	2085	77,79	0,74	2278	96,22	1,08
UDMA_AU_ref	2088	91,32	1,03	2283	104,01	1,48
UDMA_AU_17,5	2092	99,51	1,75	2273	125,3	2,13

DIAGNOSIS No3: LIBS analysis of the laser plume plasma

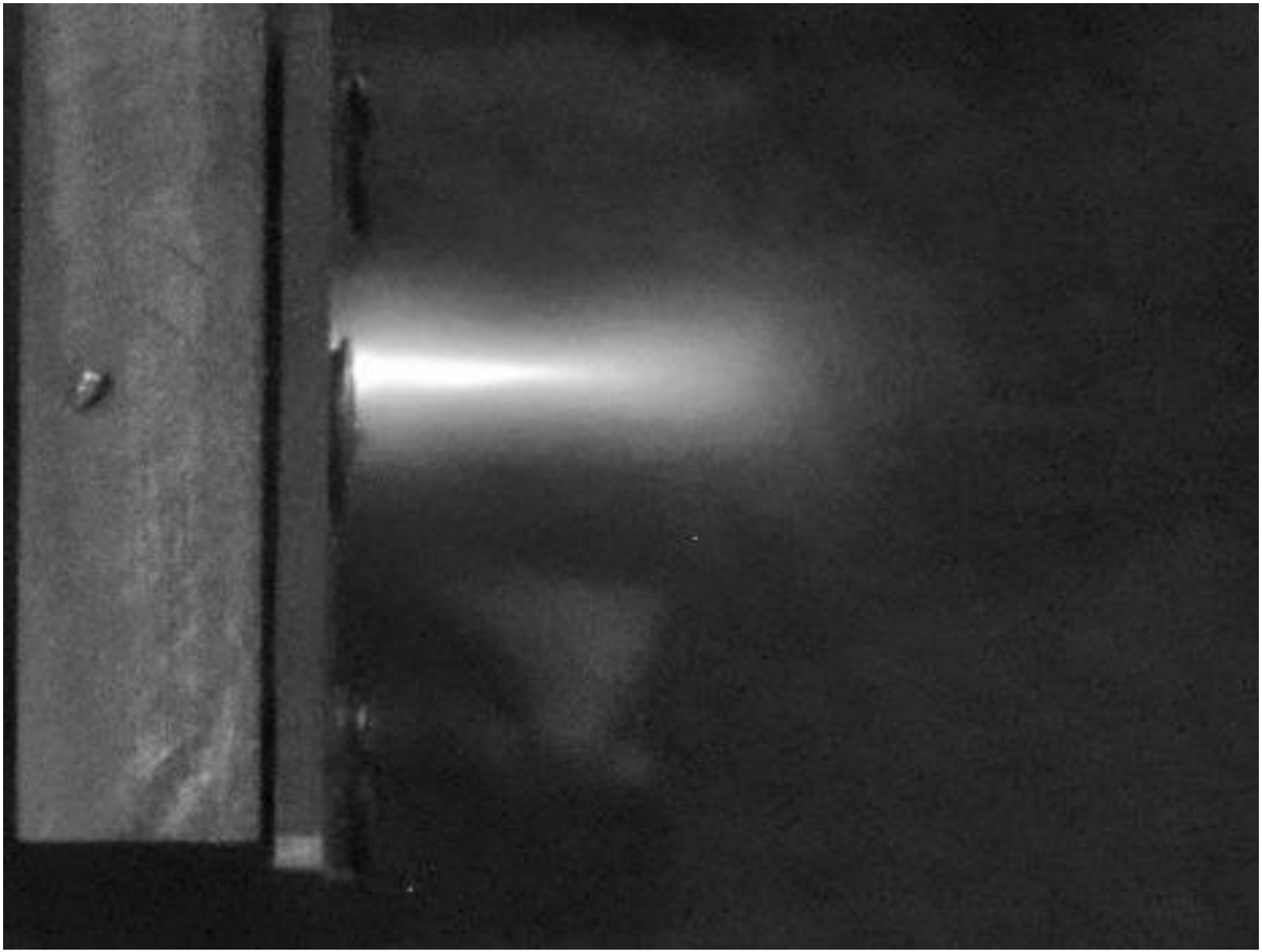

PHOTO OF A LASER SHOT INDUCED PLASMA PLUME

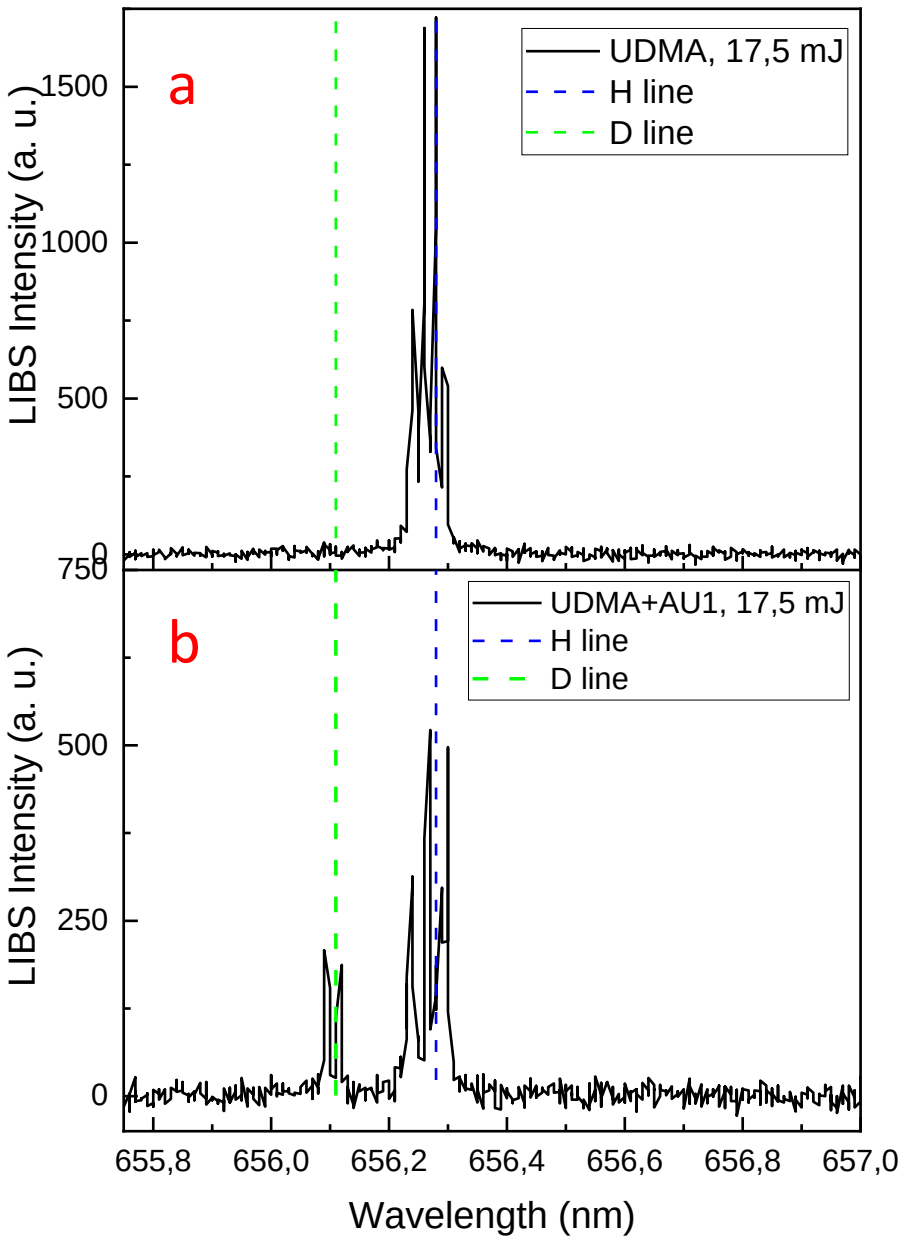

D/(2D+H): 6.8%

2D+H is the total number of hydrogen atoms before the transmutation process

Number of deuterium atoms per 17.5mJ shots: ~1.76×10^{15}

CONCLUSIONS 2.

LSPP-s (as well as SPP-s) exist at extreme high fields (at least in the femtosecond excitation domain)

The laser pulses penetrate into the samples at these high intensities

The short (femtosecond) laser pulses open the field to study phenomena out of thermal equilibrium.

„Classical" specroscopic studies (e.g. Raman and LIBS spectroscopy) can be explored to diagnose the physical processes

SOME PRELIMINARY RESULTS OF THESE STUDIES WILL BE PRESENTED IN SOME OTHER TALKS OF THIS CONFERENCE

I THANK YOU FOR YOUR ATTENTION